PHILOSOPHICAL TRANSACTIONS OF THE ROYAL SOCIETY A MATHEMATICAL, PHYSICAL & ENGINEERING SCIENCES

A review of melt migration processes in the adiabatically upwelling mantle beneath oceanic spreading ridges

P. B. Kelemen, G. Hirth, N. Shimizu, M. Spiegelman and H. J. Dick

Phil. Trans. R. Soc. Lond. A 1997 **355**, 283-318
doi: 10.1098/rsta.1997.0010

A review of melt migration processes in the adiabatically upwelling mantle beneath oceanic spreading ridges

By P. B. Kelemen[1], G. Hirth[1], N. Shimizu[1], M. Spiegelman[2] and H. J. B. Dick[1]

[1] *Woods Hole Oceanographic Institution, Woods Hole, MA 02543, USA*
[2] *Lamont Doherty Earth Observatory, Palisades, NY 10964, USA*

We review physical and chemical constraints on the mechanisms of melt extraction from the mantle beneath mid-ocean ridges. Compositional constraints from MORB and abyssal peridotite are summarized, followed by observations of melt extraction features in the mantle, and constraints from the physical properties of partially molten peridotite. We address two main issues. (1) To what extent is melting 'near-fractional', with low porosities in the source and chemical isolation of ascending melt? To what extent are other processes, loosely termed reactive flow, important in MORB genesis? (2) Where chemically isolated melt extraction is required, does this occur mainly in melt-filled fractures or in conduits of focused porous flow?

Reactive flow plays an important role, but somewhere in the upwelling mantle melting must be 'near fractional', with intergranular porosities less than 1%, and most melt extraction must be in isolated conduits. Two porosity models provide the best paradigm for this type of process. Field relationships and geochemical data show that replacive dunites mark conduits for focused, chemically isolated, porous flow of mid-ocean ridge basalt (MORB) in the upwelling mantle. By contrast, pyroxenite and gabbro dikes are lithospheric features; they do not represent conduits for melt extraction from the upwelling mantle. Thus, preserved melt extraction features do not require hydrofracture in the melting region. However, field evidence does not rule out hydrofracture.

Predicted porous flow velocities satisfy ^{230}Th excess constraints (*ca.* 1 m yr^{-1}), provided melt extraction occurs in porous conduits rather than by diffuse flow, and melt-free, solid viscosity is less than *ca.* 10^{20} Pa s. Melt velocities of *ca.* 50 m yr^{-1} are inferred from patterns of post-glacial volcanism in Iceland and from ^{226}Ra excess. If these inferences are correct, minimum conditions for hydrofracture may be reached in the shallowest part of melting region beneath ridges. However, necessary high porosities can only be attained within pre-existing conduits for focused porous flow. Alternatively, the requirement for high melt velocity could be satisfied in melt-filled tubes formed by dissolution or mechanical instabilities.

Melt-filled fractures or tubes, if they form, are probably closed at the top and bottom, limited in size by the supply of melt. Therefore, to satisfy the requirements for geochemical isolation from surrounding peridotite, melt-filled conduits may be surrounded by a dunite zone. Furthermore, individual melt-filled voids probably contain too little melt to form sufficient dunite by reaction, suggesting that dunite zones must be present before melt extraction in fractures or tubes.

Phil. Trans. R. Soc. Lond. A (1997) **355**, 283–318
Printed in Great Britain

1. Introduction

(a) Residual peridotites are not in equilibrium with MORB

MORB forms by partial melting of adiabatically decompressing mantle peridotite beneath spreading ridges (Allègre *et al.* 1973; McKenzie & Bickle 1988). Nevertheless, MORB is not in equilibrium with residual peridotite (harzburgite and lherzolite). For example, MORB is not saturated in orthopyroxene (Opx) at Moho pressures, whereas Opx is a major constituent of mantle peridotites dredged and drilled from the mid-ocean ridges (hereafter, 'abyssal peridotites') and mantle peridotites in ophiolites. Liquids parental to MORB are saturated with Opx at pressures greater than 8 kbar (O'Hara 1965; Stolper 1980; Elthon & Scarfe 1980), greater than 15 km below the Moho. In addition, most abyssal peridotites and mantle peridotites in ophiolites are strongly depleted in light rare earth elements (REE) and other highly incompatible elements, and are therefore far from trace element equilibrium with MORB (Johnson *et al.* 1990; Johnson & Dick 1992; Kelemen *et al.* 1995*b*; Dick & Natland 1996; Ross & Elthon 1997*a*, *b*). These observations indicate that MORB is a mixture that preserves evidence for partial melting of mantle peridotite over a range of pressures, much higher than the pressure at the base of the crust (Klein & Langmuir 1987; Salters & Hart 1989; Kinzler & Grove 1992).

(b) MOST melt extraction is in chemically isolated conduits of focused flow

Polybaric, near-fractional melting models closely approximate the composition of MORB and residual peridotites (Johnson *et al.* 1990). To produce large fractionations between light and heavy REE, and between elements such as Ti/Zr and Lu/Hf in residual peridotites, small melt fractions must be segregated from their sources and mixed to form MORB. To preserve these fractionations, and to produce disequilibrium between melt and Opx at low pressure, most melts must be transported to the crust without re-equilibration with surrounding peridotite. Diffuse porous flow of large amounts of melt through residual peridotite from the source to the crust would lead to extensive chemical reaction, decreasing or erasing trace element fractionation (Spiegelman & Kenyon 1992; Hart 1993; Iwamori 1993). Reaction would also bring derivative liquids close to low pressure Opx saturation (Kelemen 1990); such liquids cannot comprise a significant fraction of MORB. Thus, focused flow of melt in spatially restricted conduits is required for MORB extraction from the mantle. However, diffuse, reactive flow of small amounts of melt, at low melt/rock ratios, cannot be ruled out.

(c) Melt inclusions and magma conduits

Shimizu and co-workers discovered extensive trace element heterogeneity in glass inclusions hosted in magnesian olivine crystals within MORB. These include 'ultra-depleted melts' (UDM), silica-rich, Opx-saturated liquids that are strongly light REE depleted, and have high Ti/Zr, consistent with derivation by low pressure partial melting of the most depleted abyssal peridotite (Sobolev & Shimizu 1993). This observation substantiates the hypothesis that MORB is a mixture of melts derived from variably depleted sources at different depths beneath ridges.

Light REE enriched melts are also found in olivine-hosted glass inclusion suites (Sobolev & Shimizu 1994). These were originally believed to represent small degree melts of garnet lherzolite. Such an interpretation would place strong constraints on the nature of magma conduits beneath ridges. They would, in some instances, be re-

quired to retain unmixed melt fractions derived from the greatest depths. However, heavy REE ratios in the inclusions are inconsistent with derivation of melts directly from garnet lherzolite. Instead, Shimizu (1997) proposed that melts of garnet peridotite reacted with spinel peridotite to produce the observed liquid compositions, and Sobolev (1997) proposed that observed liquids are mixtures with an unusually large proportion of garnet lherzolite melts.

Alternatively, light REE enriched melt inclusions at slow spreading ridges can be explained by melt/rock reaction in the shallow mantle, without any involvement of garnet. Rising magma encounters the base of the conductive geotherm at about 20 km depth (Sleep 1975). Reaction between primitive MORB and depleted harzburgite under conditions of decreasing liquid mass can produce light REE enriched liquids with a flat heavy REE slope, the same as melt inclusions from the Mid-Atlantic Ridge (figure 1). This model is not unique, but we present it to emphasize that the presence of light REE enriched melt inclusions places few constraints on melt extraction beneath ridges.

(*d*) *'Near-fractional' melting models*

As noted in § 1 *b*, geochemical data on abyssal peridotite have been explained as the result of fractional melting. However, there are significant discrepancies between clinopyroxene (Cpx) compositions predicted for pure fractional melting and observed incompatible element ratios in Cpx in abyssal peridotite (Johnson & Dick 1992; Sobolev & Shimizu 1993; Iwamori 1993). For instance, La/Sm, Ce/Sm and Zr/Ti ratios are higher, at a given Nd/Sm, than predicted by purely fractional melting. This discrepancy has been explained by 'near-fractional' melting processes characterized by a constant intergranular porosity in the rock during melting, and/or reactive porous flow during melt extraction. For example, in 'incremental melting', fixed fractions of melt are periodically extracted and melt extraction is chemically isolated. Johnson *et al.* (1990) estimated that melt fractions in this model must be less than 1%, assuming that the increment is the same throughout the melting region. In 'continuous' or 'dynamic melting', a threshold intergranular porosity must be achieved before melt extraction. With continued melting, this threshold porosity is retained in the rock, and melt extraction is chemically isolated (Langmuir *et al.* 1977; Maaloe & Scheie 1982; Johnson & Dick 1992; Sobolev & Shimizu 1993). Johnson & Dick (1992) found that a retained porosity of 0.1–0.5% fits the abyssal peridotite data best, assuming that the intergranular porosity is the same throughout the melting region. Models in which melt reacts or mixes with residual peridotite have also been proposed (Elthon 1992; Iwamori 1993) – again assuming that this amount is constant throughout the melting region. These models provide a close fit to the data provided that the amount of reaction or mixing is small.

(*e*) *Not all melting is necessarily 'near-fractional'*

To explore the flexibility of constraints from the abyssal peridotite data on melting and melt extraction, we investigated two models with non-constant intergranular porosity. In the first, melting occurs in a closed system (batch melting) until a melt fraction (porosity) of 7 wt% is reached; then the intergranular porosity drops to zero, and melting is fractional. This is an example of a model in which a percolation threshold must be achieved before melt is extracted. The threshold is higher in pyroxene-rich lherzolite in the initial stages of melting, and drops to zero in depleted

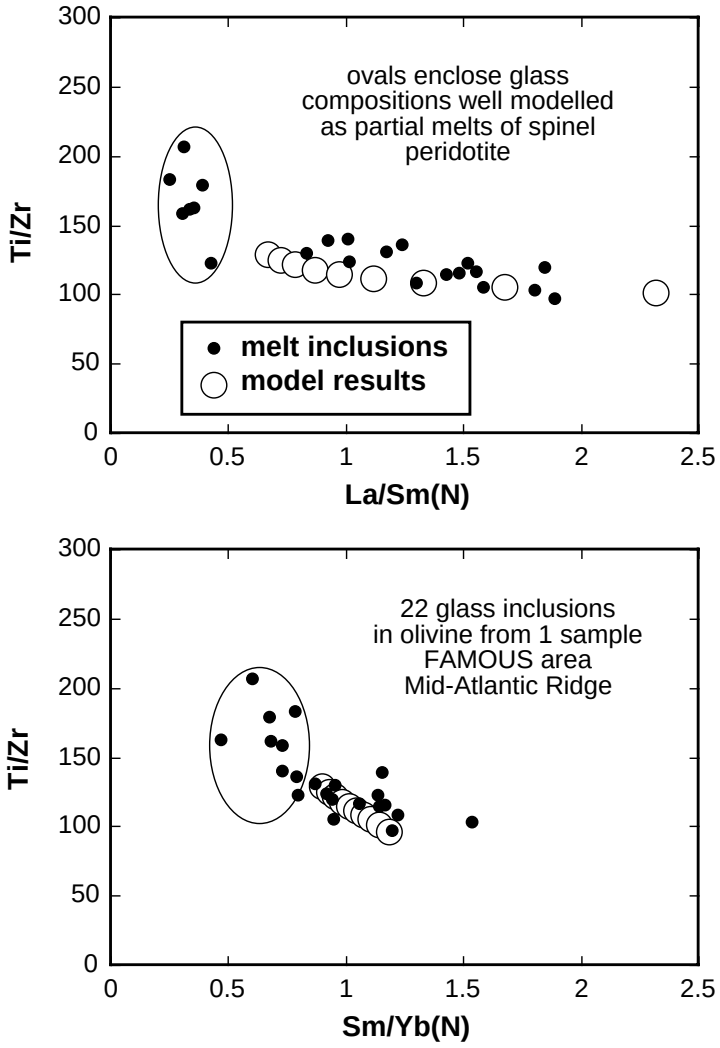

Figure 1. Melt/rock reaction between MORB and shallow mantle peridotite can form light rare earth element (REE) enriched liquids such as those in melt inclusions in olivine along the Mid-Atlantic Ridge (Shimizu 1997). To model melt/rock reaction, we used the DePaolo (1981) formalism, with a MORB initial liquid (chondrite normalized La, Ce, Nd, Sm, Eu, Gd, Dy, Er, Yb: 6, 7, 8, 9, 9.5, 10, 10, 10, 10), and a depleted harzburgite solid reactant (2×10^{-13}, 2×10^{-4}, 0.019, 0.18, 0.25, 0.27, 0.34, 0.39, 0.51) with 63 olivine: 23 orthopyroxene: 9 clinopyroxene: 5 spinel, produced by 15% fractional melting of MORB source mantle (melting model described in caption for figure 2). The mass of solid reactants/solid products, Ma/Mc, was set at 0.97, for liquid mass is decreasing slightly as a result of conductive cooling near the base of the lithosphere. Solid phase proportions were held constant. Results are plotted for values of F (fraction of initial liquid mass) from 1 to 0.1. Ovals enclose glass compositions well modelled as partial melts of spinel peridotite. The melt/rock reaction model accounts well for all other glass compositions.

harzburgites near the top of the melting column (Nicolas 1986). The correspondence of model results to the abyssal peridotite data is remarkably close (figure 2).

We were surprised by this result, and so tested an equally extreme model in which melting is fractional until 7 wt% melt is extracted, after which an additional 13%

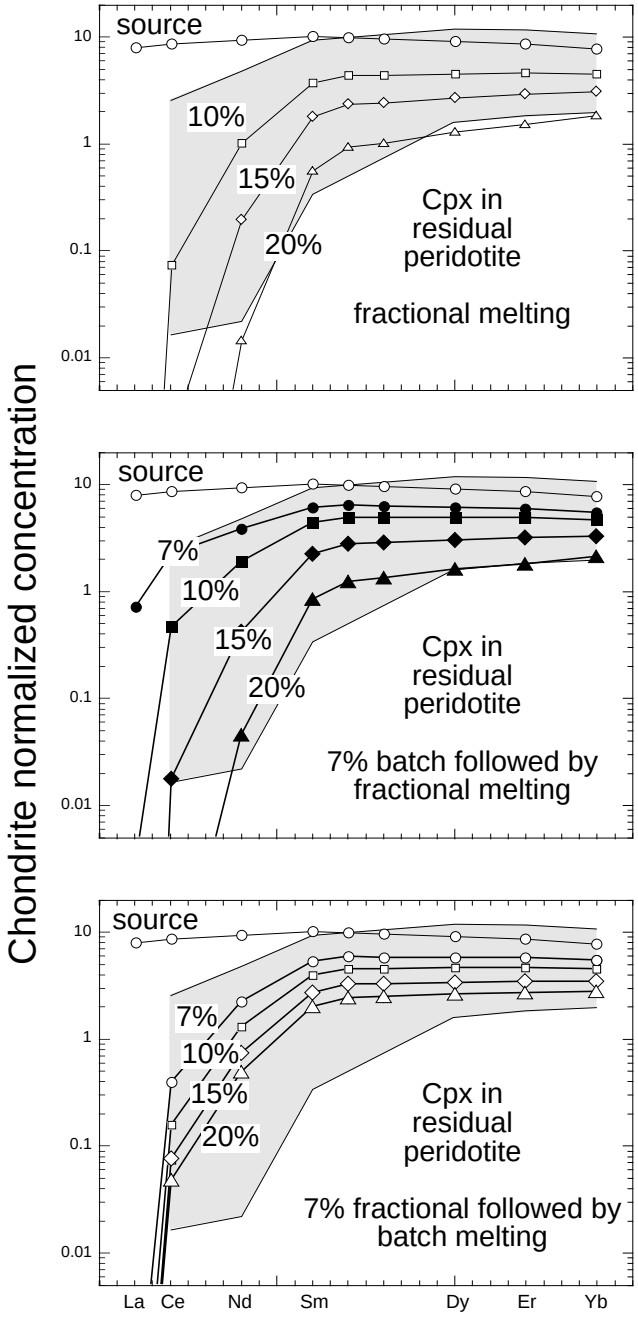

Figure 2. Calculated REE in clinopyroxene (Cpx) in residues of partial melting of mantle peridotite in spinel lherzolite facies, with various different combinations of batch and fractional melting. Grey shaded area illustrates the range of REE in Cpx in abyssal peridotites (Johnson *et al.* 1990; Johnson & Dick 1992). No unique combination of batch and fractional melting processes is required to account for the abyssal peridotite data. However, an interval of near-fractional melting, on the order of 3 wt%, is required to produce large light/heavy REE fractionation. Calculations used the methods of Gast (1968) and Shaw (1970), melt and source modes from Kelemen *et al.* (1992), partition coefficients compiled by Kelemen *et al.* (1993), and initial peridotite composition from Shimizu (1997), with Yb = 2× chondritic concentration.

batch melting occurs. This model also provides a good fit to the peridotite data. Our point is not that either model is correct, but to emphasize that if the porosity (or the amount of reactive porous flow) is variable, rather than constant over the entire melting column, there are a rich variety of melt extraction mechanisms that produce residues similar to abyssal peridotite. Therefore, the *maximum* intergranular porosity and the *integrated* amount of reactive flow during partial melting and melt transport is poorly constrained. However, Cpx compositions in abyssal peridotites require that, *at some point in the melting process, near-fractional melting did occur*. As a rule of thumb, the minimum amount of near-fractional melting, F, must be greater than or equal to the smallest crystal/liquid distribution coefficient for elements which are fractionated in residual peridotites during the melting process, such as Nd and Sm. Thus, $\geqslant 3\%$ near-fractional melting is apparently required to account for the abyssal peridotite data.

(*f*) *U/Th isotopic disequilibrium and reactive flow at the base of the melting regime*

U/Th isotopic disequilibrium in MORB indicates that melt extraction in the presence of garnet involves porous flow at intergranular porosities less than 0.2% (McKenzie 1985; Williams & Gill 1989; Beattie 1993*a*, *b*; Spiegelman & Elliot 1993; Iwamori 1994; Richardson & McKenzie 1994; Lundstrom *et al.* 1995). Since fractionation of highly incompatible elements such as U/Th requires very small intergranular porosities, melt must leave its source almost as fast as it forms. In near-fractional melting models, this constraint reduces the solid residence time for radioactive U. Since garnet is apparently required to hold more U than Th in the source, and virtually all the U is in the liquid after 1–2% melting, even in the presence of garnet, excesses of ^{230}Th are only produced in the initial stages of fractional melting. U/Th isotopic disequilibrium has also been explained by reactive porous flow over some portion of the melt extraction region (Spiegelman & Elliott 1993; Lundstrom *et al.* 1995). Reactive porous flow incorporates both small intergranular porosities and long ingrowth times in the source region. Reactive porous flow could produce ^{230}Th excesses anywhere that garnet is present in the melting region.

Hirth & Kohlstedt (1996) concluded that small amounts of H_2O-rich melt begin to form at depths of 120–70 km beneath mid-ocean ridges with 'normal' mantle potential temperatures (1300 °C). This is in addition to the possible formation of carbonate-rich melt at greater depth (Plank & Langmuir 1992, and references therein). The proportions of volatile-rich melts will be small, buffered by the limited available H and CO_2. Thus, small amounts of melt will be produced over a large depth interval, at *ca.* 0.1% kbar^{-1}. This hypothesized deep melting regime must be strikingly different from the anhdyrous melting regime that produces the bulk of MORB. It is plausible that reactive porous flow in the deep, volatile-rich melting regime produces the observed excesses of ^{230}Th in MORB.

(*g*) *Reactive flow also occurs in the shallow mantle*

Based on U/Th isotopic disequilibrium, reactive porous flow of melt may be important near the base of the melting regime (§ 1 *f*). In a similar way, Th/Ra disequilibrium data suggest that reactive flow may occur near the top of the melting regime. ^{226}Ra has a half life of about 1600 years. If ^{226}Ra disequilibrium were produced by melting of garnet lherzolite, rapid ascent of magma would be required, providing a strong constraint on transport models. However, reactive porous flow could produce ^{226}Ra isotopic disequilibrium in the absence of garnet, even at shallow

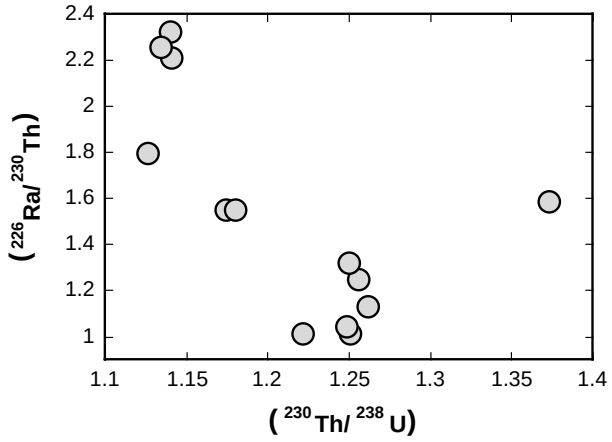

Figure 3. Plot of data for ^{226}Ra and ^{230}Th excesses in MORB. There is a negative correlation, which suggests that the excesses are produced by different processes and/or at different depths. Data are those compiled by Lundstrom *et al.* (1995) and Sims (1995).

depths, provided that Ra is more incompatible than Th for spinel lherzolite/liquid (Ra partitioning data are not available). Thus, ^{226}Ra excess excess may be created in a different part of the melting regime than ^{230}Th excess. This inference is supported by data that show a negative correlation between ^{230}Th/^{238}U excess and ^{226}Ra/^{230}Th excess in MORB, implying that two separate geochemical regimes produce the two different excesses (figure 3).

An unequivocal example of reactive porous flow is the formation of plagioclase lherzolites sampled by dredging along mid-ocean ridges. Many plagioclase lherzolites cannot be entirely residual in origin, and can be interpreted as residual peridotites that were refertilized by crystallization of plagioclase, Cpx, and olivine from melt migrating by porous flow (Dick 1989; Elthon 1992). Similar 'impregnated peridotites' are common near the crust–mantle transition zone in the Oman ophiolite (Rabinowicz *et al.* 1987; Ceuleneer & Rabinowicz 1992; Boudier & Nicolas 1995).

Insight into the scale of reactive flow is provided by geochemical variability in abyssal and ophiolite peridotites. Average peridotite compositions on the 1000 km^2 scale follow predicted melting trends (figure 4). However, abyssal and ophiolite peridotites from on the 100 km^2 scale show 'decoupled' major and trace elements; locally, there is no correlation between trace element ratios and Cpx abundance. In general, decoupled major and trace element variation can result from (1) redistribution of major elements by dissolution and precipitation reactions (Quick 1981; Kelemen 1990; Kelemen *et al.* 1992), combined with (2) 'cryptic' metasomatism in which trace elements are redistributed by liquid in major element equilibrium with host peridotite (Menzies *et al.* 1985; Bodinier *et al.* 1990). Both of these processes involve liquid migrating by reactive porous flow. Additional hypotheses and evidence for reactive porous flow in ophiolite peridotites have been presented by Gregory (1984), Takazawa *et al.* (1992), Ozawa (1994), Ozawa & Shimizu (1995) and Quick & Gregory (1995).

(*h*) *Geophysical data indicate that average porosity is low*

The conclusion that intergranular porosity must be small over an interval of $\geqslant$3% melting (§ 1 *e*) is supported by geophysical data. There are anomalously slow shear wave velocities, attributable to the presence of melt, beneath the East Pacific Rise

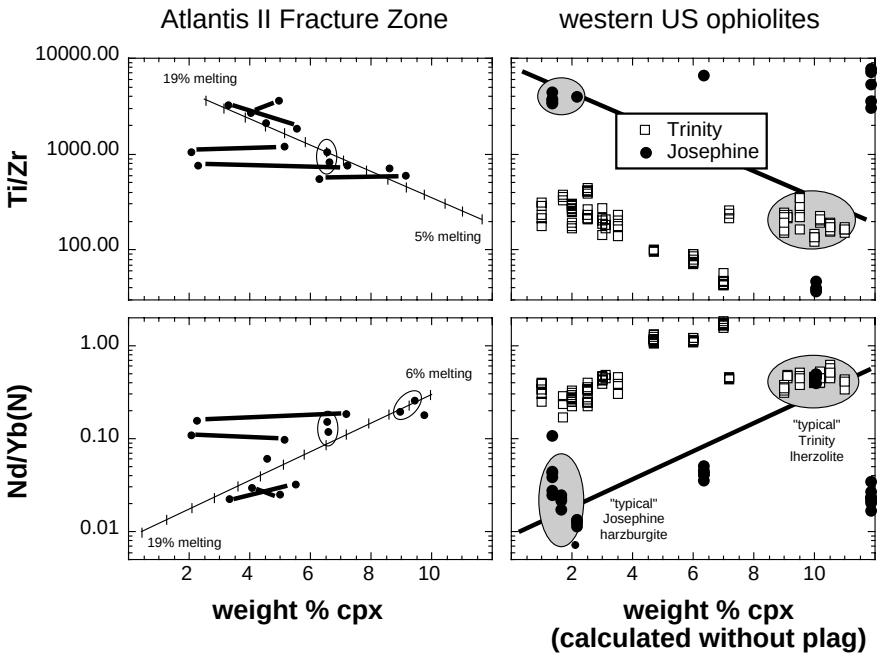

Figure 4. Trace element contents and proportions of Cpx in abyssal peridotites (Johnson & Dick 1992) and in mantle peridotites from the China Mountain area in the Trinity peridotite (Quick 1981*a*, *b*; Kelemen *et al.* 1992) and the western half of the Josephine peridotite north of the Oregon border (Dick 1976 and our unpublished data). For the abyssal peridotite data, samples obtained from the same dredge haul are connected by bold, straight lines or enclosed within ovals. For Trinity data, Cpx mode was calculated for plagioclase-free peridotite using plagioclase = Cpx + Opx + spinel − olivine. Curves on each diagram are residues of melting calculated by Johnson & Dick (1992). For both abyssal peridotites and ophiolites, the mode varies dramatically within a single dredge haul or peridotite massif (*ca.* 1 km^2 for dredge hauls, 100 km^2 for Trinity samples, 200 km^2 for Josephine samples). In contrast, trace element ratios are relatively constant on this scale. The wide spread in Cpx mode for the Trinity and Josephine reflects ubiquitous but volumetrically minor, centimetre- to metre-scale variation; 'typical' peridotites are relatively uniform within each massif, and the two massifs are distinctly different. If one were to 'dredge' the Trinity, one would likely obtain a lherzolite with mild light REE depletion. In contrast, dredging of the Josephine would likely yield a harzburgite with extreme light REE depletion.

and the Mid-Atlantic Ridge (Forsyth 1992; Forsyth *et al.* 1996). However, the intergranular porosity is small, between 3 and 6.5% at 45 km if melt is in grain-boundary tubes, and less than 1% if melt is in grain boundary films. Since a substantial proportion of melt is present in films rather than tubes (Waff & Faul 1992; Jin *et al.* 1994; Hirth & Kohlstedt 1995*a*; Faul 1997), the interconnected, intergranular porosity is probably less than 3%. The shear wave data do not rule out the presence of additional melt in isolated pockets. However, analysis of gravity from the southern East Pacific Rise indicates that little melt is present in interconnected pores or isolated pockets (Magde *et al.* 1995). Thus, the geophysical data support the inference from geochemical observations that the average intergranular porosity in the melting column is small, and that melt extraction by porous flow on some length scale must be chemically isolated.

(*i*) *Conclusion: two porosity models are needed*

The foregoing sections present evidence for (1) chemically isolated melt transport by focused flow of melt in spatially restricted conduits (§ 1 *b*), and (2) diffuse, reactive porous flow (§§ 1 *f*, *g*) beneath spreading ridges. This apparent paradox can be understood in the context of two porosity models (Wang 1993). In these models, the bulk of the liquid flux is in highly permeable conduits, but a significant quantity of geologically important trace elements are derived from processes involving a much smaller flux of liquid moving by diffuse porous flow in the interstices between these conduits.

2. Melt migration features in the mantle section of ophiolites

Localized melt migration is essential in extraction of MORB from the mantle. In this section, we review data on localized melt migration features at the outcrop scale in ophiolites and their analogues in abyssal peridotite. We concentrate on data from the Oman ophiolite, because several observations demonstrate that it formed at an oceanic spreading centre. The crustal section includes a continuous layer of sheeted dikes. The main lava series and the dikes are tholeiitic lavas with REE and trace element contents similar to MORB (Alabaster *et al.* 1982). In detail, REE and other incompatible trace elements in the Oman lavas are lower, at a given Cr concentration, than in 'normal' MORB. However, the similar compositions of Oman lavas and MORB indicate that the processes that formed the ophiolite were similar to processes operating at mid-ocean ridges. On the basis of radiometric age data, the lack of crustal thickness variation, and other geological observations, it is probable that the ophiolite formed at a fast-spreading ridge (Tilton *et al.* 1981; Nicolas 1989).

(*a*) *Mantle dunites*

(i) *Dunites are conduits for MORB transport in the asthenosphere*

Dunites are rocks composed of more than 90% olivine, with lesser amounts of spinel and, locally, pyroxene. For brevity, we use only the term dunite to refer to such rocks, and the term peridotite to refer only to rocks with less than 90% olivine. 'Discordant' dunites are the most common magmatic feature in the mantle section of ophiolites. We distinguish between 'mantle dunites' and dunites in the crust–mantle transition zone of ophiolites, which may have a different origin. Mantle dunites comprise 5–15% of the exposed mantle section in Oman (Boudier & Coleman 1981; Lippard *et al.* 1986, table 3.6). They preserve sharp, irregular contacts that are locally discordant to banding and crystallographic lineation in the harzburgite (Lippard *et al.* 1986, p. 53). Because harzburgites and most dunites have a foliation parallel to the palaeo-Moho, it is inferred that both were transposed by corner flow beneath a spreading ridge. Thus, transposed dunites were formed in upwelling mantle beneath a ridge.

Geochemical data suggest that dunites mark conduits for focused flow of MORB through the adiabatically upwelling mantle. In Oman, a substantial proportion of dunites contain minor Cpx. Kelemen *et al.* (1995*b*) demonstrated that these Cpx have REE in equilibrium with liquids similar to MORB and to the dikes and lavas that form the upper crust of the ophiolite. In addition, spinel in dunites has high molar Cr/(Cr+Al), denoted 'Cr#' and high Ti, like most spinels in primitive MORB. As in Oman, Cpx in medial gabbro selvages within dunites formed in shallow mantle at the East Pacific Rise (sampled at Hess Deep) are in trace element equilibrium

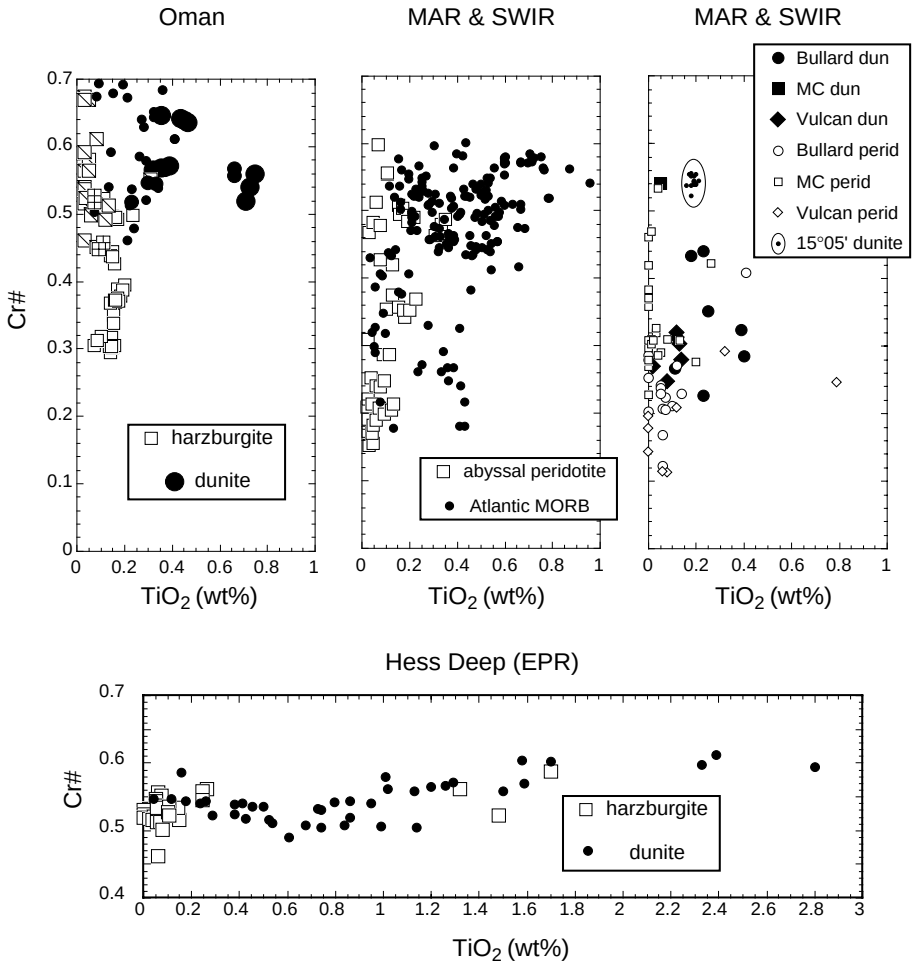

Figure 5. Compositions of spinel in dunites and associated peridotites from the Oman ophiolite (Pallister & Hopson 1981; Augé 1987; Kelemen *et al.* 1995*b*), and from abyssal peridotites dredged and drilled from the Mid-Atlantic Ridge (MAR), Southwest Indian Ridge (SWIR), and East Pacific Rise (Hess Deep – EPR) (Dick & Bullen 1984; Allan & Dick 1996; Arai & Matsukage 1996; Dick & Natland 1996; and our unpublished data; 'MC' is an abbreviation for Marie Celeste Fracture Zone). Also shown for comparison are compositions of spinel in MORB from the Atlantic (compiled by Dick & Bullen 1984). Dunites generally have Cr/(Cr+Al), denoted 'Cr#', as high as the most depleted peridotites, but higher TiO_2 than any associated peridotites. Spinels in MORB are compositionally similar to those in dunite, and different from those in residual peridotite.

with MORB (Dick & Natland 1996). Spinels in these dunites have high Cr# and high Ti, similar to spinel in Oman dunites and in MORB (Allan & Dick 1996; Arai & Matsukage 1996; Dick & Natland 1996). Our unpublished data show that high Cr# and high Ti are also typical of abyssal dunite from the Mid-Atlantic and SW Indian Ridges (figure 5). Thus, dunites from Oman and mid-ocean ridges have spinel compositions similar to those found in MORB, supporting the notion that dunites are conduits for MORB transport. An essential caveat is that some ophiolites are polygenetic, and not all dunites in ophiolites reflect equilibration with melts similar

to MORB (Kelemen *et al.* 1992; Takazawa *et al.* 1992; Ozawa 1994; Ozawa & Shimizu 1995; Quick & Gregory 1995; Gruau *et al.* 1995; Takazawa 1996).

(ii) *Dunite dimensions*

The size distribution and proportion of dunites can be used to estimate melt/rock ratios within melt extraction conduits. The largest mantle dunites in Oman are in the Wadi Tayin massif (Hopson *et al.* 1981). We find that these are tabular, in two cases more than 200 m thick and up to 10 km long. They are locally massive, but elsewhere are anastamosing, with elongate harzburgite inclusions up to 10 m thick and 100 m long. Another large dunite, in the Hilti massif (Al Wasit geological map, Oman Ministry of Petroleum & Minerals 1987) is more than 100 m thick and more than 10 km long, sub-parallel to the Moho.

The resolution at which smaller dunites in Oman have been mapped varies. In the well-mapped Wadi Tayin massif (Fanjah, Samad and Quryat geological maps 1986), there are more than 35 dunites more than 1 km long in *ca.* 800 km^2. Most are transposed, sub-parallel to the Moho, indicating that they have undergone corner flow. Their map widths generally exceed 100 m (their true thickness ranges from 20 to 100 m). Thus , 'large' dunites comprise *ca.* 0.5% of the exposed mantle section. Smaller dunites are ubiquitous. If the estimate that dunite comprises 5–15% of the mantle section in Oman is correct (§ 2 *a* (i)), then 'small' dunite bodies must be more than 90% of this total.

Because the proportion of dunite may increase upward and toward the centre of the melting region, transposed dunites in the 10 km thick mantle section of the ophiolite may represent most or all of the dunite formed in the upwelling column. If so, and if the melting region was *ca.* 100 km deep, then dunite comprises 0.5–1.5% of the melting region. 'Large' dunites comprise *ca.* 10% of this total. If most melt flowed through dunite conduits, and the mean extent of melting was 10%, then the average melt/rock ratio in all dunites would be 20:1 to 8:1. If most melt flowed in 'large' dunites, the melt/rock ratio would be 200:1 to 80:1.

(iii) *Most mantle dunites are replacive features*

Hypotheses for the origin of mantle dunites are reviewed by Kelemen *et al.* (1995*a*, *b*), who conclude on the basis of geological and geochemical data that most dunites are replacive features, formed by dissolution of pyroxene and concomitant precipitation of olivine in magma migrating by porous flow. Please see Dick (1976, 1977), Quick (1981), Berger & Vannier (1984), Bodinier (1988), Kelemen (1990), Kelemen *et al.* (1992), and Quick & Gregory (1995) for important contributions, and Kelemen *et al.* (1995*a*, *b*) for additional references and discussion. Here, we add previously unpublished ideas.

In addition to the hypothesis that they are replacive, mantle dunites have been interpreted as fractures filled with olivine precipitated from migrating melt (i.e. 'cumulates'). However, data on $Mg/(Mg+Fe^{2+})$, denoted 'Mg#', suggests that few if any large dunites are cumulates. Compared to olivine in mantle peridotite, olivine in cumulate dunite should have lower Mg#. In fact, Mg#'s are similar in olivine from dunites and associated mantle peridotites (Kelemen 1990; Kelemen *et al.* 1995*b*). If dunites are cumulate, their limited range of Mg# indicates that they represent a very small fraction of the parental magma mass. For example, Takahashi (1992) reports less than 0.5% variation of Mg# in a tabular dunite *ca.* 10 m wide and more than 5 km long. This requires that the dunite, if cumulate, represents less than 2% of ini-

tial liquid mass, provided the initial liquid had less than 15 wt% MgO. A restricted range of Mg# is the norm for mantle dunite; it is unlikely that the combination of cooling rate and melt flux would always produce such small degrees of crystallization. Thus, high and relatively constant Mg#'s in large mantle dunites indicate that most are not cumulate. Since melt/rock reaction maintains nearly constant Mg# (Kelemen 1986, 1990), a replacive origin can explain the similar olivine Mg#'s in dunites and host peridotite, as well as their mono-mineralic composition and contact relationships.

(iv) *How much dunite can be formed by reaction? < 5% of the melting region*

The solubility of pyroxene in ascending melt is about 1 wt% kbar^{-1} of decompression (figure 3 in Kelemen *et al.* 1995*a*). The maximum amount of dunite that can be formed is 3 wt% of the mantle in the melting region, assuming the average degree of melting is 10 wt%, the average pressure of melting is 13 kbar, the pressure at the base of the crust is 3 kbar, and average peridotite has 30 wt% pyroxene. If this were the case, the average melt/rock ratio in these dunites would be 2:1 and all magmas would be saturated with Opx. However, primitive MORB is far from Opx saturation, as noted in § 1 *a*. Therefore, the melt/rock ratio must be more than 2:1. If the average melt/rock ratio were more than 100:1 (i.e. dunite proportion less than *ca.* 0.1%), the resulting magmas would be far from equilibrium with Opx and the dunite formation process would have little geochemical effect on the composition of MORB. In this case, the aggregate liquids that comprise MORB could be regarded as a mixture of polybaric partial melts. If the melt/rock ratio has an intermediate value, *ca.* 10:1 (i.e. 1% dunite), then MORB would be far from Opx saturation, but dunite formation might have other effects on the composition of MORB.

(v) *Is there a 'dunite signature' in MORB? Maybe*

As noted in § 2 *a* (iv), if the melt/rock ratio in dunite conduits is *ca.* 10, then dunite formation should have a compositional effect on MORB. In fact, MORB has characteristics unlike aggregated, polybaric partial melts that could be produced by dunite formation. Figure 6 is a plot of Ce/Yb(N) in liquids against Cr# in spinel. MORB, and liquids calculated to be in equilibrium with Oman dunites, have Ce/Yb(N) near 1, as high as in liquids in equilibrium with the least depleted abyssal peridotites. Spinel in MORB and in dunites has Cr# of about 0.6, as high as spinel in the most depleted abyssal peridotites. This reflects the fact that REE ratios in MORB record the average degree of melting of the source, while Cr# apparently records the highest degree of melting.

The apparent discrepancy in degrees of melting recorded by Cr# versus Ce/Yb(N) can be explained if liquids involved in dunite formation constitute a moderate proportion of MORB (i.e. dunites comprise *ca.* 1% of the rock). The dunite forming reaction, pyroxene + liquid → olivine + spinel + liquid, can increase the Cr-content of derivative liquids, but has little effect on REE ratios (figure 6). Pending improved models for spinel/liquid equilibria, this hypothesis must be regarded as conjectural. Alternatively, mixing of Ce-rich, Cr-poor liquid produced at small degrees of melting with Cr-rich, Ce-poor liquid produced by large degrees of melting could produce the observed MORB composition, assuming that variability of Al and Yb in mantle-derived magmas is negligible. However, what would become of magmas produced by intermediate degrees of melting? If they were added, the mixture would be in equilibrium with spinel with intermediate Cr#. Thus, the dunite hypothesis may be

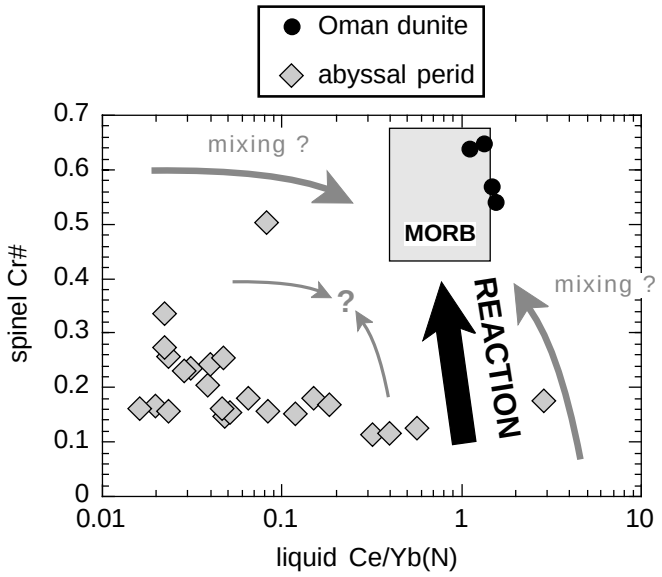

Figure 6. Calculated Cr# in spinel and chondrite normalized Ce/Yb, denoted 'Ce/Yb(N)', in liquid, illustrating that MORB may include a compositional 'signature' of dunite formation. Field for MORB is based on compiled compositions of spinels (Dick & Bullen 1984) and liquids (Langmuir *et al.* 1992). Dunite and peridotite Ce/Yb(N) were calculated from Cpx compositions and Cpx/liquid distribution coefficients of Hart & Dunn (1993). Data for Cpx in abyssal peridotites are from Johnson *et al.* (1990) and Johnson & Dick (1992), and data for Cpx in dunites are from Kelemen *et al.* (1995*b*), for Oman ophiolite samples. Mass balance calculations for dunite forming reactions yield the trend labeled 'REACTION'. For example, this trend results if peridotite and liquid have REE contents as for figure 1, peridotite has 0.5 wt% Cr_2O_3 and 3–10 wt% Al_2O_3, initial liquid has 100 ppm Cr and 15 wt% Al_2O_3, dunite has 1% spinel, melt/rock ratio is 10, ratio of peridotite reactant to dunite product is 1.1, olivine/liquid = 2 for Cr and 0.0001 for Al, and spinel/liquid = 200 for Cr and 2 for Al.

preferable. A signature of dunite formation in MORB has also been suggested based on spinel compositions (Arai & Matsukage 1996), and major element trends (Niu & Batiza 1993; Gaetani *et al.* 1995).

(vi) *The reactive infiltration instability (RII)*

Daines & Kohlstedt (1994) and Kelemen *et al.* (1995*a*) proposed that dunites originate as dissolution channels. Since pyroxene dissolution combined with olivine precipitation increases liquid mass under conditions of constant temperature or constant enthalpy (Kelemen 1990; Daines & Kohlstedt 1994), it follows that such reactions will increase magma mass – and porosity – under adiabatic conditions. Dissolution of pyroxene in olivine-saturated magma is analogous to porous flow of fluid through a partially soluble rock. Theoretical and experimental studies show that diffuse porous flow in these systems is unstable. Because initial perturbations in permeability lead to enhanced fluid flow, which in turn leads to more rapid dissolution, diffuse flow breaks down into focused porous flow through high porosity dissolution channels, elongate in the direction of fluid flow (Chadam *et al.* 1986; Hoefner & Fogler 1988; Daccord 1987). This is termed the 'reactive infiltration instability' (RII).

The RII was first considered for rigid porous media, with an initial, planar solution front normal to the direction of fluid flow. With numerical experiments (Kelemen

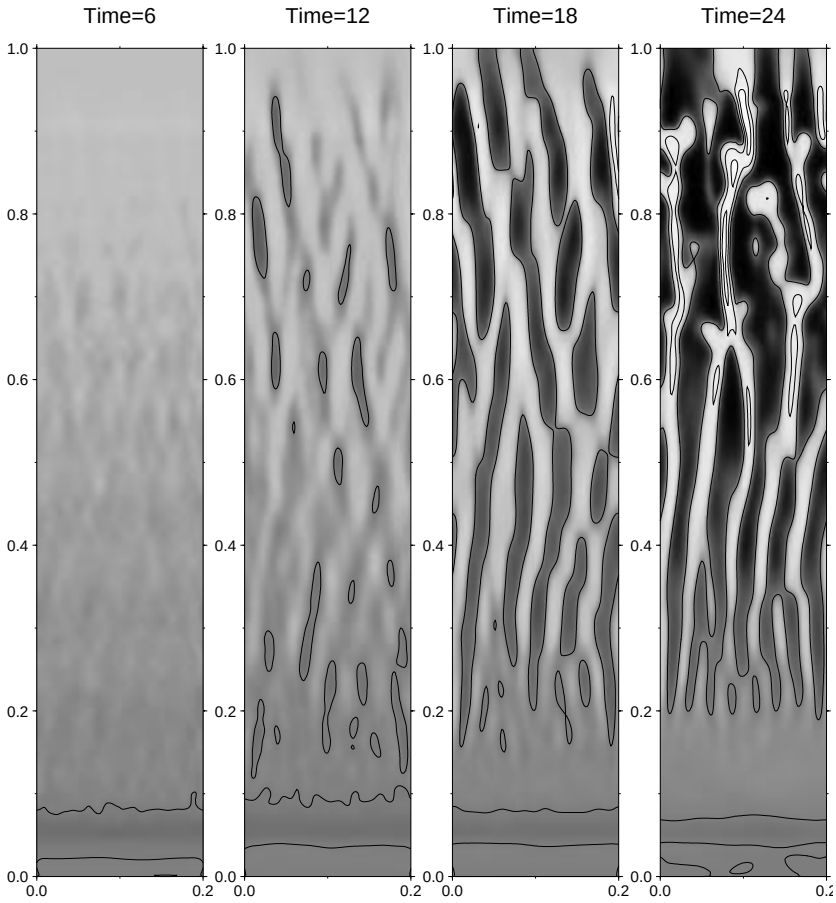

Figure 7. Evolution of porosity from a fully nonlinear calculation for porous flow in a viscously compacting, soluble medium, illustrating how high porosity dissolution channels form and coalesce. All times have the same grey scale map. Contours of 1% porosity are shown. Final frame has a minimum porosity near 0.1%, and a maximum near 3%. The minimum porosity is limited by a non-constant bulk viscosity that makes it difficult to compact very small porosities (Sleep 1988). Numerical parameters are 65×321 grid points, 36276 time steps. Boundary conditions are constant flux bottom and free-flux top with periodic (wrap-around) sides. These are preliminary results from Spiegelman *et al.* (1996).

et al. 1995*a*) and a stability analysis (Aharonov *et al.* 1995), we have shown that the RII occurs in a solubility gradient with no initial solution front, and in viscously compacting porous media. The RII is continuously present in time and space in a solubility gradient; as long as soluble solids remain in the system, dissolution channels grow unstably. Because the solubility of peridotite in adiabatically decompressing melts increases with decreasing pressure, the RII can occur throughout the melting region.

The most obvious manifestation of dissolution reactions in the mantle is the formation of dunite by dissolution of pyroxene. However, even olivine has a finite solubility in adiabatically ascending melt, so that the RII could form high porosity channels *within* dunite. If melt supply is sufficient, this might ultimately form 'open', melt-filled tubes. Ongoing research on the RII includes investigation of branching and

coalescence of channels and partitioning of flow between dissolution channels and the surrounding matrix. Aharonov *et al.* (1995) predicted, and preliminary numerical experiments confirm, that dissolution channels coalesce downstream (upward, in the mantle), provided that solubility increases downstream (e.g. figure 7). In these calculations, where the permeability contrast between channels and matrix exceeds 1000, more than 95% of the flux is focused in dissolution channels that comprise less than 10% of the volume (Spiegelman *et al.* 1996).

(vii) *Mechanical instabilities*

Stevenson (1989) noted that in viscously deforming media, weak regions may have a slightly lower pressure than surrounding, stronger regions. Therefore, he proposed that melt will tend to flow from strong regions into weaker regions. Because melt fraction is negatively correlated with the strength of partially molten peridotite (Hirth & Kohlstedt 1995*a*, *b*), this can unstably form melt-rich shear zones within a melt-poor matrix (the 'Stevenson instability'). Similar hypotheses have been proposed by Sleep (1988). A role for mechanical focusing of melt flow is demonstrated by dunites in the Josephine peridotite that formed syn-kinematically along ductile shear zones in conductively cooled, shallow mantle at *ca.* 1100 °C (Kelemen & Dick 1995). Factors that localized melt flow probably included the Stevenson instability, anisotropic permeability due to vertical foliation in shear zones, and the RII.

(*b*) *Dikes: lithospheric features, and – in Oman – generally not formed by MORB*

Pyroxenite and gabbroic dikes are observed in the mantle section of many ophiolites. The dikes are generally discordant to the high temperature foliation in residual peridotites (Boudier & Coleman 1981; Lippard *et al.* 1986; Nicolas 1989). Formation of pyroxene and plagioclase is indicative of crystallization from evolved, low temperature liquid. Such liquids form by crystal fractionation due to conductive cooling. We infer that the dikes, as well as tabular dunites with medial pyroxenites (Trinity peridotite, Quick 1981*b*), formed off-axis, in lithosphere with a conductive geotherm.

In Oman, compositional data demonstrate that many gabbronorite and pyroxenite dikes in the mantle section were not conduits for MORB extraction. Cpx in 6 of 8 dikes from the Wadi Tayin massif are strongly light REE depleted (figure 8), and have high Ti/Zr (Farrier *et al.* 1997). In these respects they are identical to Cpx in peridotites from the same massif (Kelemen *et al.* 1995*b*) and abyssal peridotites (Johnson *et al.* 1990). The dikes represent small amounts of crystallization of melt derived from a source similar to the Oman harzburgites. These melts had REE contents very different from MORB. Instead, the melts were similar to 'ultra-depleted' melts (UDM, § 1 *c*) observed in glass inclusions within some olivine phenocrysts in MORB (Sobolev & Shimizu 1993).

A 'cumulate' origin for Wadi Tayin dikes is indicated by high Mg# in Cpx (83–95 mol%) and high anorthite in plagioclase (85–95 mol%), demonstrating that all dikes contained little or no 'trapped liquid' (Farrier *et al.* 1997). Thus they are not asthenospheric melt pockets that cooled to form gabbroic rocks in the lithosphere. Most of the dikes are websterites or gabbronorites (Opx-rich). Thus, the liquids were saturated in Opx, similar to UDM and very different from MORB. We conclude that melts which formed the Wadi Tayin dikes were derived from a source similar to the surrounding harzburgite, and that the dikes are shallow, lithospheric features. Further, their similarity to UDM – the lowest pressure melt in the polybaric mixture comprising MORB – indicates that UDM may be transported from the shallow

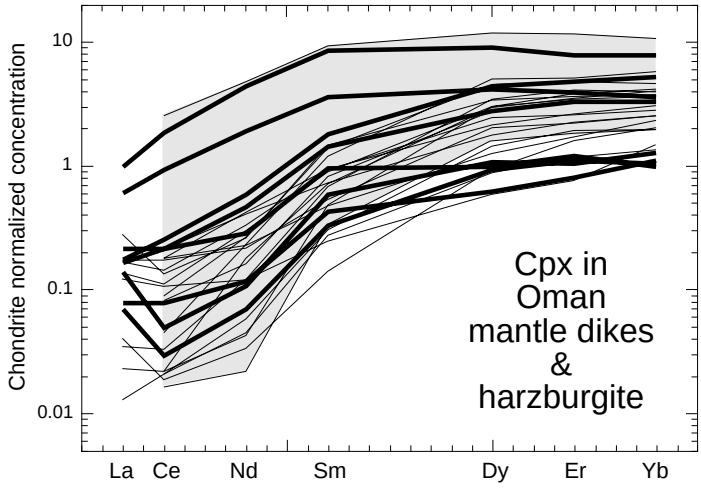

Figure 8. REE contents of Cpx in gabbronorite and websterite dikes from the Wadi Tayin massif of the Oman (bold lines), compared to Cpx in harzburgite from the same massif (light lines) and in abyssal peridotite (shaded field). Six of eight dikes analysed had Cpx REE contents different from Cpx in equilibrium with MORB, and very similar to Cpx in residual peridotites, suggesting that the dikes are formed by crystal fractionation from liquids derived by low pressure partial melting of highly depleted peridotite. Data for dikes from Farrier *et al.* (1997), for Oman peridotite from Kelemen *et al.* (1995*b*), and for abyssal peridotite from Johnson *et al.* (1990) and Johnson & Dick (1992).

mantle in dikes. If UDM have a transport mechanism different from other melts, this could explain why UDM are occasionally found as glass inclusions within olivine in MORB (Sobolev & Shimizu 1993), and why some cumulate gabbros from mid-ocean ridges have strongly light REE depleted compositions (Ross & Elthon 1993, 1997*a*, *b*).

There are mantle dikes that did form in equilibrium with MORB-like liquids. As noted in § 2 *a* (i), Cpx in medial gabbro within dunite from the shallow mantle lithosphere at Hess Deep are in trace element exchange equilibrium with normal MORB (Dick & Natland 1996). Similarly, gabbroic dikes and sills that formed in equilibrium with melts similar to MORB are found in the upper 1–2 km of the mantle section below the crust in the Maqsad region of the Oman ophiolite (Benoit *et al.* 1997; Kelemen *et al.* 1997). Thus, on the basis of limited data, it seems that most gabbroic dikes more than 2 km below the base of the crust in the Oman ophiolite formed off-axis, from depleted liquids similar to UDM, whereas most gabbroic dikes and sills close to the base of the crust form from liquids similar to MORB.

Dikes in peridotite from the Mid-Atlantic Ridge have been recovered by dredging, submersible sampling and drilling (Cannat 1996; Cannat & Casey 1995). Most of these are different from gabbroic dikes of the Oman ophiolite, extending to more evolved compositions with enriched minor and trace element compositions. Gabbroic dikes from the Mid-Atlantic Ridge formed in equilibrium with liquids more enriched in incompatible elements than MORB, by a combination of melt/rock reaction and extensive crystal fractionation within cold, lithospheric mantle peridotite.

(*c*) *Are dunites associated with cracks? Some are. (Most are not?)*

Most mantle dunites have a replacive origin. However, there might have been 'cryptic fractures' in the centre of most or all dunites during their formation, resulting in a kind of 'uncertainty principle' for geologists seeking to determine whether fractures play an important role in melt extraction from the asthenosphere. Melts rising adiabatically in a crack will not become saturated in any solid phase. Such a crack might close, leaving no trace, when liquid is no longer present. In this sense, field observations do not require asthenospheric melt flow in cracks, but they cannot be used to rule it out.

The tabular nature of many dunites has been used to infer that they are related to fractures. Indeed, tabular dunites with a medial pyroxenite, common in the Lanzo peridotite (Boudier & Nicolas 1972), the Horoman peridotite (Takahashi 1992) and the Trinity peridotite (Quick 1981*b*), may be porous reaction zones around melt-filled fractures (Nicolas 1986). Similar features have also been recovered at Hess Deep, in drill core from the crust–mantle transition zone (Dick & Natland 1996). However, mass balance constraints (§ 3 *f*) suggest that it is unlikely that tabular dunites form around individual fractures. While the tabular geometry of many dunites probably does not arise from reactive porous flow alone (though Tait *et al.* (1992) report tabular dissolution channels), tabular dunites could form as a result of the RII combined with anisotropic permeability in peridotite and/or an anisotropic stress distribution (see § 2 *a* (vii) and § 4 *d*). Cracks may form within dunite, due to their high intergranular porosity and large grain size (§§ 3 *b*, *f*). This is most likely near the base of the lithosphere.

(*d*) *Chromitites: focused flow, but not necessarily in asthenospheric fractures*

Chromitites are composed of more than 50% massive chromian spinel. In ophiolites, they are enclosed within dunite, rather than peridotite. Chromitites are indicative of focused melt flow (Leblanc & Ceuleneer 1992). Because the solubility of Cr-spinel is low in silicate melts, chromitites must have scavenged Cr from 300 to 400 times their mass in liquid. Thus, the integrated melt/rock ratio for both chromitites and some of the surrounding dunites is more than 300. The fact that chromite crystallizes in massive concentrations, despite its low concentration in magmas, reflects sluggish kinetics for chromite nucleation compared to crystal growth. Basaltic magmas must commonly be supersaturated in chromite, but still able to transport Cr until they come into contact with chromite that has already nucleated.

Chromitites have been interpreted to form in melt-filled voids by magmatic sedimentation (Lago *et al.* 1982; Nicolas 1986, 1990). Alternatively, they may form in porous media. Sedimentation was suggested by 'nodular' chromitites (ellipsoid chromite grains a few centimetres in diameter), resembling a grain-supported conglomerate. However, in 'orbicular' chromitites, also common, chromite ovoids are not in contact and are 'hollow', with olivine cores. Some show alternating rings of chromite and olivine (Nicolas 1989, fig. 10.12*c*). These are similar to orbicular structures in granites (Wang & Merino 1993, fig. 1) and concretions formed during diagenesis in porous rocks (Wang & Merino 1995).

Lago *et al.* (1982) and Nicolas (1986) found that flux calculations based on suspension of chromite crystals by magmatic flow were consistent with the rate of magmatic accretion of the crust, and suggested that this supported the hypothesis that melt extraction occurs in hydrofractures extending from near the base of the melting regime

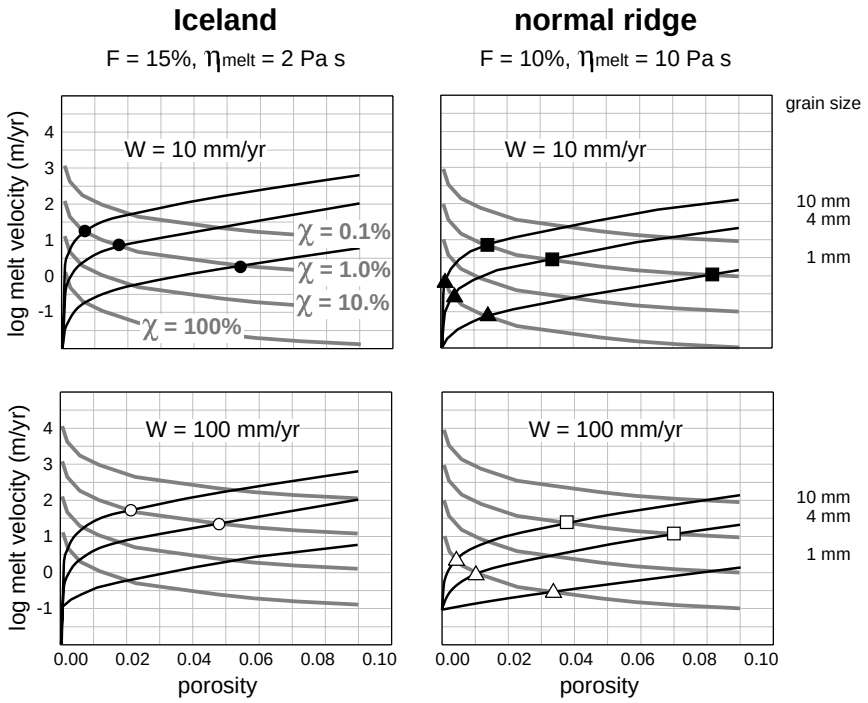

Figure 9. Velocities, relative to the Earth's surface, for melts migrating by porous flow in the mantle. In general, porous flow velocities in the mantle can be high enough to satisfy melt velocity constraints for mid-ocean ridges based on U/Th isotopic disequilibrium, the magmatic response to Icelandic deglaciation, and the steady state melt flux. Velocities calculated using Darcy's law with permeability from Cheadle (1993) are shown as black, solid lines for solid grain sizes of 10, 4 and 1 mm. Values are shown for two melt viscosities, 2 Pa s ('Iceland') and 10 Pa s ('normal ridge'), and two solid upwelling velocities, 10 and 100 mm yr^{-1}. Also shown as light grey lines are solutions to a one-dimensional melt flux equation for mid-ocean ridges, $w = WF/(\phi\chi)$, in which w and W are melt and solid velocities, ϕ is the porosity, F is the average fraction of melting (taken to be 15% for Iceland and 10% for normal ridges) and χ is the proportion of melt conduits. Intersections between the curves specify melt velocity and porosity of steady-state flow for a given grain size and proportion of melt conduits. Circles, squares and triangles highlight specific intersection points; these points are also shown in figure 10.

to the Moho. However, we show in § 3 *a* that porous flow can also supply magma at the rate of magmatic accretion of the crust (7000 m^2 per 10–100 years per unit length of ridge). Even accepting that chromitites are magmatic sediments, it does not follow that they form in fractures in the asthenosphere. They could form in shallow mantle. Most chromitites are found within a few kilometres of the Moho. High melt velocities do not require flow in a pipe or a tabular opening with a large vertical dimension (Spera 1980; Lago *et al.* 1982). In addition, even if chromitites form in melt-filled voids spanning tens of kilometres in the asthenosphere, these voids could be formed by the RII (§ 2 *a* (vi)), mechanical instabilities (§ 2 *a* (vii)), or a combination of these processes, as well as by fracture.

(*e*) *Summary*

Dunites and chromitites mark conduits for chemically isolated extraction of MORB within the ascending mantle. Dunites are replacive features formed by dissolution of

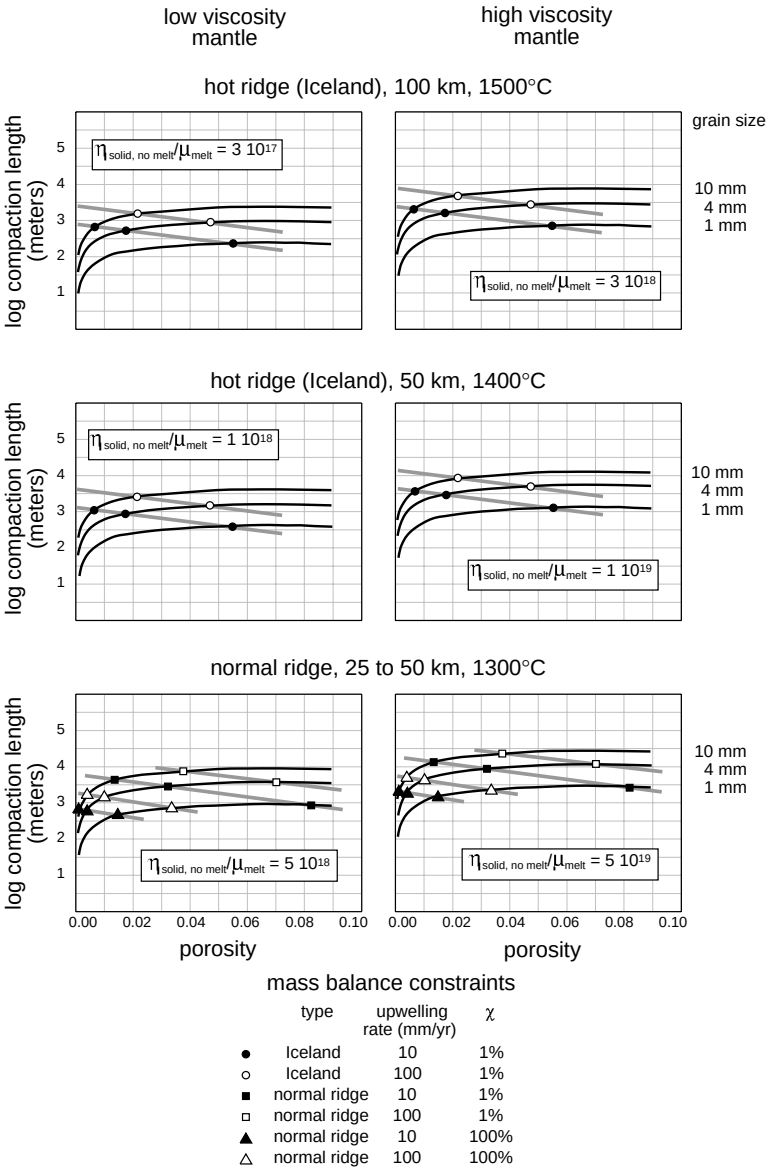

Figure 10. Calculated compaction lengths for a variety of mantle temperatures, solid and melt viscosities, and solid grain sizes, shown as black, solid lines. Also shown as light grey lines are porosities and compaction lengths consistent with the one-dimensional, steady state melt flux equation for mid-ocean ridges (from figure 9). In general, these results suggest that hydrofracture is unlikely in the region of adiabatic upwelling beneath mid-ocean ridges. The likelihood of hydrofracture is enhanced if melt flow is restricted to a few, high porosity conduits within coarse-grained rocks. If mantle viscosities are as high as allowable given current geophysical data, then the minimum compaction length for hydrofracture, 10^4 m, is exceeded for conduits of focused flow ($\chi \leqslant 1\%$) within rocks with an average grain size more than 4 mm.

pyroxene in melt ascending along conduits of focused porous flow. Fractures within dunites in the asthenosphere are not required, but cannot be ruled out on the basis

of geological data. In contrast, pyroxenite and gabbro dikes are lithospheric features and do not provide information about melt transport in the asthenosphere.

3. Constraints from physics

(*a*) *Is porous flow fast enough to account for melt velocity estimates? Yes.*

Four types of melt velocity estimates are available for oceanic spreading ridges. Two come from U-series disequilibria, a third is based on geological observations in Iceland, and a fourth is based on simple mass balance constraints for melt extraction from a one-dimensional column.

Excesses of ^{230}Th (half life of *ca.* 75 000 years) and ^{226}Ra (*ca.* 1600 years) in fresh, zero age MORB indicate that melt transport from the point where these excesses grew to the surface was rapid compared to the half life of ^{230}Th and ^{226}Ra. Since garnet is apparently required to hold more U than Th in a solid phase (Beattie 1993*a*, *b*), excesses of radiogenic ^{230}Th are produced only in the deepest part of the melting region, below the garnet–spinel peridotite transition, perhaps 75 km beneath the crust (Spiegelman & Elliot 1993; Iwamori 1994; Richardson & McKenzie 1994; Lundstrom *et al.* 1995). It has been proposed that garnet pyroxenite contributes significantly to the composition of MORB (Chabaux & Allègre 1994; Hirschmann & Stolper 1996). Since garnet is stable to lower pressures in pyroxenite bulk compositions than in peridotites, ^{230}Th excesses could theoretically be produced by reactive porous flow in garnet pyroxenites at depths less than 75 km. However, pyroxenite bodies in mantle peridotite samples always form tabular bands. Reactive porous flow is unlikely to be restricted to garnet pyroxenite bands within spinel peridotite.

Thus, ^{230}Th disequilibrium requires melt transport rates *ca.* 75 km per 75 000 years, or 1 m yr^{-1}. If ^{226}Ra disequilibrium must form in the presence of garnet, then melt velocities must be *ca.* 50 m yr^{-1}. However, as noted in § 1 *g*, ^{226}Ra disequilibrium may be formed in the shallow mantle; in this case it is not a strong constraint on mantle melt transport velocities. Jull & McKenzie (1996) report an outpouring of basaltic magma associated with deglaciation in Iceland. They infer that melt was produced by decompression due to deglaciation, throughout the melting region extending to perhaps 100 km depth, and reached the surface within 2000 years. This requires melt velocities *ca.* 50 m yr^{-1}. However, other explanations are possible for the post-glacial volcanism; e.g. long term storage of magma in a lower crustal reservoir.

In a one-dimensional, upwelling column, steady state melt velocity is related to fraction of melting and solid upwelling by $w = WF/\phi$, where w and W are melt and solid velocities and F and ϕ are the fraction of melting and the porosity (Spiegelman 1993*c*). If virtually all melt flow is focused in conduits, this may be modified to $w = WF/(\phi\chi)$, where χ is the proportion of conduits. As noted in § 2 *a* (iv), if melt flow conduits are dunite dissolution channels, then chemical data require that χ be $\leqslant$3%. Geochemical data (§ 2 *a* (v)) suggest that χ is *ca.* 1%. A value of *ca.* 1% may also be inferred from the proportion of dunite in the Oman ophiolite (§ 2 *a* (ii)). However, note that if more than 90% of the melt is transported in 10% of dunite conduits, and dunite conduits comprise 1% of the melting region, $\chi \approx 0.1\%$.

Solutions for $F = 15\%$ (Iceland) and 10% (normal ridges), and $\chi = 100$, 10, 1 and 0.1% are plotted as wide, shaded curves in figure 9. These can be compared to melt velocities inferred from post-glacial volcanism in Iceland and from U/Th

disequilibrium at normal ridges. If mantle upwelling beneath Iceland is comparable to the spreading rate and $\phi > 0.1\%$, then melt velocities of order $50\,\mathrm{m\,yr^{-1}}$ are only achieved for $\chi \leqslant 1\%$. Beneath a normal, slow spreading ridge (upwelling rate of $10\,\mathrm{mm\,yr^{-1}}$, $\phi > 0.1\%$), χ must be less than 100% to reach a melt velocity of $1\,\mathrm{m\,yr^{-1}}$. Thus melt extraction must occur in spatially restricted channels ($\chi < 1$) in order for steady state flow velocities to satisfy velocity constraints.

The mass balance constraints on melt velocity can also be compared to buoyancy-driven, porous flow velocities (solid lines in figure 9), calculated using Darcy's law with permeability estimated by Cheadle (1993), as reported in McKenzie (1989). We use the Cheadle estimates (similar to Von Bargen & Waff 1986) because of uncertainty in extracting permeability from experiments by Riley & Kohlstedt (e.g. 1991), Daines & Kohlstedt (1993), and Faul (1997). Permeability varies with grain size as well as porosity. Olivine and pyroxene grain size in the mantle is generally 3–10 mm (Mercier 1980). Mantle dunites are coarser-grained than surrounding peridotites. Dunites commonly have an average grain size *ca.* 10 mm. In syn- and post-kinematic dunites, olivine has irregular shapes, interfingering with adjacent crystals (Nicolas 1989, fig. 2.7*a*; Kelemen & Dick 1995, fig. 7*B*). The irregular grain shapes preserved in the dunites are not consistent with static, sub-solidus grain growth. We therefore infer that the grain size in dunites is larger than that in surrounding peridotites during melt flow in the mantle.

Buoyancy-driven, permeability-based melt velocities beneath Iceland and normal mid-ocean ridges are shown as black solid lines in figure 9 for solid upwelling at 10 and $100\,\mathrm{mm\,yr^{-1}}$. Melt viscosity is inversely proportional to the average pressure of melting (Kushiro 1986). Beneath Iceland, with melt viscosity of 2 Pa s and mantle upwelling similar to the spreading rate, melt velocities of $1\,\mathrm{m\,yr^{-1}}$ (fast enough to preserve ^{230}Th excess) can be attained at ϕ of 0.2 and less than 0.1% for grain sizes of 4 and 10 mm. To achieve melt velocities of $50\,\mathrm{m\,yr^{-1}}$, inferred from Icelandic deglaciation volcanism, ϕ of 7 and 2% are required for the same grain sizes. Beneath a normal, slow-spreading ridge, with melt viscosity of 10 Pa s and passive upwelling, melt velocities of $1\,\mathrm{m\,yr^{-1}}$ are attained at ϕ of 1.5 and 0.2% for 4 and 10 mm grains.

In the previous paragraph we have not incorporated mass balance. Since the total melt flux is limited by the rate of decompression melting, high liquid flow velocities at high porosity cannot be sustained at steady state because they require more liquid than is produced. Therefore, assuming *both* (1) that the Cheadle (1993) permeability estimates are accurate and (2) that the one-dimensional, steady state flux calculation is a good approximation, steady-state melt velocities and porosities are defined by the intersections of the mass balance curves and the permeability-based curves in figure 9. These intersections specify melt velocity and porosity given values of grain size, W, F and χ. With $F = 10\%$ and $\chi = 1\%$, the requirement that melt moves at more than $1\,\mathrm{m\,yr^{-1}}$ beneath Iceland is easily satisfied; for example if the grain size is 4 mm, ϕ must be *ca.* 1.7%. However, with $F = 10\%$ and $\chi = 1\%$, melt velocities from the deglaciation constraint ($\geqslant 50\,\mathrm{m\,yr^{-1}}$) can only be satisfied if channels have a grain size more than 20 mm and $\phi \lesssim 0.2\%$. These grain sizes are larger than generally observed, even in dunite. Alternatively, if $\chi = 0.1\%$ (e.g. conduits are 1% of the melting region but a subset of 10% of conduits carries 90% of the melt flux) then melt velocities of $50\,\mathrm{m\,yr^{-1}}$ require grain size of 10 mm and $\phi \approx 2\%$.

Beneath a normal, slow spreading ridge, with $\chi = 1\%$, the requirement from ^{230}Th excess that melt moves at more than $1\,\mathrm{m\,yr^{-1}}$ is satisfied, for example, with grain size of 4 mm and $\phi \approx 3.3\%$. If $\chi = 10\%$, grain size must be greater than *ca.* 4 mm and

$\phi \lesssim 1\%$. However, if ^{226}Ra disequilibrium forms in the presence of garnet, required melt velocities of 50 m yr^{-1} beneath a slow spreading ridge with $\chi = 1\%$ are only attained at unreasonably large grain sizes. For a reasonable grain size of 10 mm, χ must be less than 0.02% and $\phi \gtrsim 6\%$.

Note that, in all cases discussed in this section, most conduit porosities required to satisfy melt velocity constraints are higher than source porosities required to produce U-series disequilibrium (*ca.* 0.1%), and higher than source porosities required for the interval of 'near-fractional' melting necessary to account for abyssal peridotite REE compositions. However, there is no reason to assume that conduit porosities and source porosities should be equal.

(*b*) *Can hydrofracture occur in adiabatically ascending mantle? Maybe, but if so, then only in pre-existing conduits.*

It has been argued that hydrofracture is unlikely in the viscously deforming, partially molten upper mantle (Stevenson 1989). The reasoning is that the mantle can deform viscously at differential stresses considerably lower than the tensile strength of the solid matrix. However, hydrofractures may also form if the melt pressure exceeds the confining pressure (σ_3) by a value equal to the tensile strength, even when the differential stress is low. The *maximum possible* ΔP (melt pressure, σ_3) due to melt buoyancy in a viscously compacting solid matrix is of the order $\Delta\rho g\delta_c$, where $\Delta\rho$ is the difference in density between melt and solid, g is the gravitational constant, and δ_c is the compaction length (McKenzie 1984). The compaction length is defined as

$$\sqrt{k_\phi(\zeta + \tfrac{4}{3}\mu_s)/\mu_1},$$

where ζ and μ_s are the bulk viscosity (deformation due to ΔP) and shear viscosity (deformation due to $\sigma_1 - \sigma_3$) of the partially molten matrix, k_ϕ is the permeability, and μ_1 is the melt viscosity. The values of ζ and μ_s are difficult to determine from experimental deformation data. Note that the larger of the two will dominate in determining the compaction length. We denote this larger value as $\eta_{\text{solid w/melt}}$, assume that experimental constraints on the influence of melt on viscosity determine this quantity, and rewrite a simplified expression for compaction length as

$$\sqrt{k_\phi(\eta_{\text{solid w/melt}})/\mu_1}.$$

The maximum value of ΔP would be attained in a porous system that suddenly started to compact, or in a compacting system beneath an overlying obstruction in the permeability. Because the compaction process acts to minimize pressure differences between solid and liquid, steady state stresses in continuously compacting systems without an overlying obstruction are smaller than this value (Spiegelman 1993*a*, *b*).

These calculations are for buoyancy-driven flow. Where forced flow drives melt from a broad region into a narrow zone, as may occur at the base of the crust beneath a spreading ridge, melt pressures may be higher. However, note that some coalescence of melt flow beneath ridges is driven by 'suction', i.e. low melt pressure (§ 4 *d*). Thus the effect of forced flow on melt pressure is uncertain, and remains a topic of continuing research.

Unfortunately, our understanding of processes that control magma fracturing in viscous materials is limited. However, a combination of constraints derived from the

rock mechanics literature and from deformation experiments on peridotite provides an estimate for the tensile strength of partially molten mantle rocks. In most experiments, samples are enclosed in metal capsules, which prevents melt from migrating out of the aggregate. The melt pressure in this case is roughly equal to the confining pressure, although it may be as high as the mean pressure. Thus, the effective confining pressure is very low, which enhances the formation of fractures.

Experiments show evidence for melt-enhanced brittle deformation of peridotite at differential stresses greater than 500 MPa (Bussod & Christie 1991). Together with an assumption that the effective confining pressure in these experiments was *ca.* 0, this result can be used to estimate the uniaxial compressive strength of partially molten peridotite. For comparison, numerous experiments conducted on similar compositions at stresses as high as 250 MPa show no evidence for brittle failure (Beeman & Kohlstedt 1993; Hirth & Kohlstedt 1995*b*). Griffith failure criteria indicate that the tensile strength of a brittle rock is 1/8 of the uniaxial compressive strength, in general agreement with experimental observations (Scholz 1990), although values between 1/10 and 1/20 are observed (Paterson 1978). We use a value of 1/10 as a minimum estimate for the tensile strength of partially molten mantle (i.e. 500/10 = 50 MPa). The value of 1/10 is justified because the fracture energy of viscous materials is generally high as a result of crack-tip blunting (i.e. crack-tip stresses are reduced by plastic deformation). With a *minimum* strength of 50 MPa, and of 500 kg m^{-3}, a compaction length *greater than* 10^4 m is required for hydrofracture.

Estimates for the compaction length as a function of porosity are shown for different grain sizes and values of the viscosity ratio $\eta_{\text{solid w/melt}}/\mu_1$ in figure 10. We have included the influence of melt on the viscosity of the solid using experimental data on partially molten dunites (Hirth & Kohlstedt 1995*a*, *b*). Data on the viscosity of the partially molten aggregate from both the dislocation and diffusion creep regimes are well fit by the relationship

$$\eta_{\text{solid w/melt}} = \eta_{\text{no melt}} \exp(-45\phi),$$

where $\eta_{\text{no melt}}$ is the viscosity of the melt free aggregate, and ϕ is porosity (Hirth & Kohlstedt 1997). As in § 3 *a*, permeabilities were calculated using Cheadle (1993). As in figure 9, we also show constraints imposed by mass balance for a one-dimensional melting column, which allow us to specify grain size and porosity for a given proportion of melt flow conduits, denoted χ.

Beneath Iceland, we estimate that the melt-free mantle viscosity is between 6×10^{17} and 6×10^{18} at a depth of 100 km and between 2×10^{18} and 2×10^{19} at 50 km. These values were calculated using experimental flow laws (Chopra & Paterson 1984; Hirth & Kohlstedt 1996), assuming that the melting region is H_2O-free and that deformation is accommodated by dislocation creep. As in § 3 *a*, melt viscosity beneath Iceland is taken to be 2 Pa s. The minimum compaction length for hydrofracture, on the order of 10^4 m, is only approached beneath Iceland if the higher mantle viscosity estimate is used, grain size is on the order of 10 mm, and porosities are greater than 3% (figure 10). Recall that for Iceland, melt velocities implied by ^{230}Th excess, 1 m yr^{-1}, can be attained with $F = 15\%$, $W = 10$ mm yr^{-1}, $\chi = 1\%$, grain size of 4 mm, and $\phi = 1.7\%$ (§ 3 *a*). At these conditions compaction lengths will be $< 10^4$ m beneath Iceland, even in the high viscosity mantle case. This result is fairly general for $\chi \geqslant 1\%$. However, melt velocities inferred from post-glacial volcanism, 50 m yr^{-1}, can be attained with $F = 15\%$, $W = 10$ mm yr^{-1}, $\chi = 0.1\%$, grain size of 10 mm, and $\phi = 2\%$. In the high viscosity case, these conditions imply a compaction length

close to 10^4 in the shallow part of the upwelling mantle. Thus, hydrofracture might be possible in the upper part of the melting regime in Iceland, provided that (1) melting is already focused in high ϕ channels with coarse grains, (2) mantle viscosity is high, and (3) the post-glacial burst of volcanism was produced by melting due to deglaciation.

Beneath a normal mid-ocean ridge, where the mantle is cooler, the melt-free solid viscosity is estimated to be between 5×10^{19} and 5×10^{20} over the interval from 25 to 50 km. Note that the commonly used value of around 1×10^{19} is estimated for an asthenospheric channel beneath a rigid plate (Hager 1991) where viscosities may be lower than in the melting region under ridges, due to the presence of dissolved hydrogen in mantle minerals outside the melting region (Hirth & Kohlstedt 1996). The melt viscosity beneath a normal ridge will be close to 10 Pa s.

For normal mid-ocean ridges, we show solutions to the mass balance equations, with $\chi = 100$ and 1%, and mantle upwelling of 10 and 100 mm yr^{-1}. Diffuse porous flow ($\chi = 100\%$) is restricted to very low porosities, permeabilities and compaction lengths, and therefore cannot satisfy melt velocity constraints or produce hydrofracture. Larger grain size and/or higher porosity can satisfy velocity constraints, but lead to compaction lengths $> 10^4$ m with the higher mantle viscosity estimates. For example, the melt velocity requirement from ^{230}Th excess is satisfied for $F = 10\%$, $W = 10$ mm yr^{-1}, $\chi = 1\%$, grain size of 4 mm, and $\phi = 3\%$, corresponding to a compaction length of *ca.* 10^4 m in the high viscosity case. For melt velocities *ca.* 50 m yr^{-1}, inferred from Th/Ra isotopes if ^{226}Ra excess is produced at the base of the melting column, we found that for a grain size of 10 mm, χ must be less than 0.02% and $\phi \gtrsim 6\%$ (§ 3 *a*). Even for low estimates of mantle viscosity, these values lead to a compaction length approaching 10^4 m.

In summary, the conditions for hydrofracture may be approached beneath Iceland and normal mid-ocean ridges, but only if the pressure difference between liquid and solid is close to the maximum possible value, and if flow is previously focused into high porosity channels composed of coarse-grained rock. Thus, coarse-grained dunite conduits with high porosities could undergo hydrofracture. However, recall that (1) 10^4 m is the estimate of the *minimum* length of a porous column sufficient for hydrofracture, (2) the *maximum possible* ΔP in a compacting system is $\Delta\rho g\delta_c$, and (3) the maximum ΔP will be approached only if compaction starts suddenly in a previously static system or if there is an overlying drop in permeability. An overlying drop in the permeability is likely only in the shallowest parts of the melting region beneath mid-ocean ridges, at the spinel–plagioclase peridotite transition (Asimow *et al.* 1995) and/or at the base of the conductively cooled lithosphere (Kelemen *et al.* 1996).

(*c*) *Would a percolation threshold increase melt pressure? Probably not.*

Nicolas (1986, 1990) has proposed that permeability in fertile lherzolite is limited (see Toramaru & Fujii 1986; Faul 1997), so that a large intergranular porosity is created in ascending mantle until a 'percolation threshold' is suddenly exceeded over a large vertical distance. This scenario would serve to minimize the effect of compaction, which tends to decrease solid–liquid pressure differences to less than $\Delta\rho g\delta_c$ over time. It is unclear why a percolation threshold should be attained suddenly over a large vertical distance. One can imagine an arbitrary initial condition in which an upwelling column above the solidus is devoid of melt. Over time, decompression melting could produce a large vertical distance with constant porosity in this column.

However, beneath the region of constant porosity and above the solidus, this process must form a region with non-constant porosity, decreasing gradually with depth to a porosity of zero at the solidus. After the overlying column with constant porosity passed through the percolation threshold, the mantle beneath the interconnected column, with porosities smaller than the percolation threshold, would still retain melt. This leads to a steady state in which partially molten peridotite becomes interconnected over a small vertical interval at a fixed height above the solidus, the point where the melt fraction exceeds the percolation threshold. Thus, it is unclear how a large column of partially molten peridotite can suddenly become interconnected in an actively upwelling mantle system. However, as outlined in § 3 *b*, increasing grain size and melt flux in porous flow channels as they develop might gradually cause liquid overpressure to approach the tensile strength of partially molten peridotite. Whereas Nicolas (1986) has proposed that dunites form around fractures, in the scenario envisioned in § 3 *b*, fractures would form within porous dunite conduits. And, although this process does not include any role for a percolation threshold, it could give rise to a periodic hydrofracture process similar in other respects to that envisioned by Nicolas (1986, 1990).

(*d*) *Cracks from above?*

Fowler & Scott (1997) have proposed that fractures originating in the lithosphere may propagate downward into the viscous, partially molten mantle, initiating melt-filled cracks. The central point is that, even when the mantle is 'too weak' for hydrofractures to form in situ, brittle fractures nucleated in the lithosphere may propagate too fast for viscous dissipation to relieve stress concentrations, and therefore may penetrate to arbitrary depths. It is unclear whether fractures initiated in this way can tap a large enough area of partially molten peridotite by suction to form melt-filled conduits.

(*e*) *Closed, melt-filled conduits in porous media are not chemically isolated*

The past few sections have concentrated on physical mechanisms for melt extraction in the upwelling asthenosphere beneath ridges. Hydrofracture seems unlikely to arise if porous melt transport is diffuse, but hydrofracture may occur under some circumstances within conduits for focused porous flow. In addition, as noted in § 2 *a* (vi), the RII may be capable of producing melt-filled conduits without hydrofracture. Formation of liquid-filled voids as a result of dissolution has been demonstrated for rigid, soluble porous media in a variety of analogue experiments (Daccord 1987; Daccord & Lenormand 1987), and is likely to occur in viscous media as well (Kelemen *et al.* 1995*a*; Aharonov *et al.* 1995). Mechanical instabilities (§ 2 *a* (vii)) could also give rise to melt-filled voids.

Regardless of how they form, it is possible to constrain the extent of melt-filled conduits. The predicted flux in planar or cylindrical conduits is huge compared to melting and crustal production rates at ridges. Poiseuille flow in a melt-filled channel with a radius or half width of 0.5 m will have a cross-sectional flux of *ca.* 10^6 m^2 yr^{-1}, at least 1000 times greater than cross-sectional rates of oceanic crustal production (10^2–10^3 m^2 yr^{-1}). Thus, melt-filled conduits must be transient and rare. Furthermore, since the flux greatly exceeds the melt production rate, and because a conduit cannot instantaneously 'suck' all the melt from the entire melting region, it is unlikely that a melt-filled conduit could extend from the base of the melting region to the base of the crust. Therefore, transient melt-filled conduits – if they form – are

likely to be closed at both ends. For this reason, melt in such a conduit must flow outward, into the surrounding peridotite, at the top and inward, from the peridotite, at the base. Illustrations of this flow pattern, for static conduits created by dissolution in rigid porous media, are given by Kelemen *et al.* (1995*a*). Similar flow patterns can be inferred from the results of Richardson *et al.* (1996) for moving, melt-filled conduits, closed at both ends, in viscous porous media. Thus, because it intrinsically involves porous flow through surrounding rocks, magma transport in melt-filled conduits probably cannot account for the requirement of chemical isolation of melt from residual mantle peridotite (§ 1 *b*).

(*f*) *Pre-existing dunite zones around melt-filled conduits*

If melt-filled conduits pass through dunite channels, magma within them will be isolated from reaction with residual mantle peridotite (figure 11). How might this be explained? Small dunite reaction zones might form around melt-filled conduits as a result of divergent porous flow from the top of the conduit. The solubility of Opx in adiabatically ascending basaltic liquid is about 1% kbar^{-1} of decompression (§ 2 *a* (iv)). Thus a given mass of liquid rising from 90 km along an adiabatic PT gradient can convert an equal mass of peridotite containing 30% pyroxene to dunite before it becomes pyroxene saturated. To preserve liquid compositions far from Opx saturation, the mass of dunite formed/mass of liquid in the conduit must be less than 1. However, Richardson *et al.* (1996) find that porous flow from a conduit into a viscous porous wall rock penetrates the wall rock to a radial distance of about one compaction length. Compaction lengths in mantle peridotite with $\phi > 0.01\%$ may vary from 10 to 10^4 m (figure 10). Thus, liquid within a melt-filled conduit ascending over a depth interval of 50 km would undergo porous flow through a cross-sectional area of 10–500 km^2 of peridotite host rock. Either (1) conduits must have cross-sectional areas much larger than this, which is unlikely, or (2) melt-filled conduits, closed at the top and bottom, must traverse pre-existing dunite channels in order to retain liquids far from Opx saturation. Perhaps the latter scenario is plausible. In § 3 *b*, we showed how hydrofractures, if they arise, would form within pre-existing conduits for focused porous flow of melt (dunites). This is equally likely for melt-filled tubes arising from the RII and/or mechanical instabilities. Wiggins & Spiegelman (1995) have shown a tendency for three-dimensional solitary waves in viscous peridotite to repeatedly follow specific pathways of high permeability. Closed, melt-filled fractures or tubes may be very similar in their behaviour to solitary waves. A third possibility, of course, is that melt-filled fractures or tubes never form, and *all* melt is transported by focused porous flow in dunite channels.

4. Plate scale melt transport: how is melt flow focused to the ridge?

A variety of models have been proposed to explain focusing of magmatic accretion to within a few kilometres of the ridge axis at both fast and slow spreading ridges (Sleep 1984; Whitehead *et al.* 1984; Crane 1985; Rabinowicz *et al.* 1987; Phipps Morgan 1987; Spiegelman & McKenzie 1987; Scott & Stevenson 1989; Sparks & Parmentier 1991; Scott 1992; Spiegelman 1993*c*). Some aspects of these models are relevant to the physical mechanisms of melt transport.

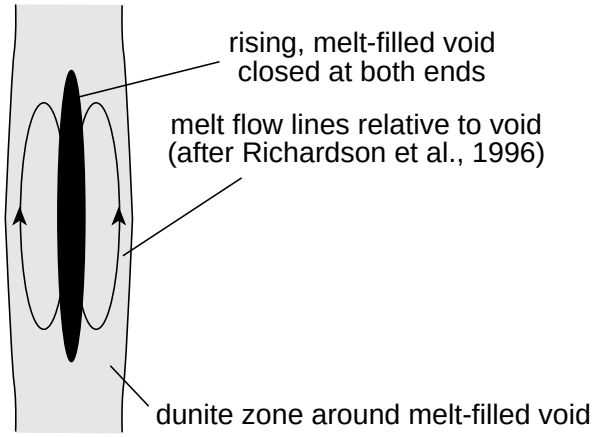

Figure 11. Schematic illustration of a melt-filled void (e.g. a fracture or dissolution channel) closed at both top and bottom, rising through partially molten, porous, viscously compacting mantle peridotite. As shown by Richardson *et al.* (1996), liquid will flow outward from the top and inward at the bottom of the void, with flow lines extending radially outward for about one compaction length. Thus, in order to maintain observed disequilibrium between melts and mantle peridotite, such melt-filled voids must move through a pre-existing dunite zone.

(*a*) *Fracture is not an effective mechanism for focusing to the ridge*

Sleep (1984) and Phipps Morgan (1987) proposed that fractures parallel to the maximum compressive stress, in upwelling mantle undergoing corner flow, will not focus melt flow, and instead will be distributed over a region 40 km wide on either side of the ridge. Nicolas (1990) questioned this, pointing out that if solid mantle upwelling itself is focused beneath the ridge due to buoyancy-driven flow, the stress field will be different from that in passive flow models. He calculated that the maximum compressive stress would be sub-horizontal (dip less than 30°) from 35 to 15 km depth, trapping melt in sills. These sills would steepen to become subvertical dikes at less than 15 km. Transport of melt in sills rising with the solid velocity over 20 km would result in net transport times longer than 10^5 years. This is too slow to account to preserve ^{230}Th excess in MORB, and therefore seems unlikely. However, if hydrofractures follow pre-existing conduits for focused porous flow, and the pre-existing conduits coalesce toward the ridge, this would produce both flow in fractures and focused crustal accretion.

(*b*) *Focused solid flow plus channels?*

Whitehead *et al.* (1984) and Crane (1985) proposed that buoyancy due to melt and to chemical depletion in decompressing mantle would give rise to focused upwelling of peridotite beneath ridges. This influential idea spawned a series of models for focused, buoyancy-driven upwelling (Rabinowicz *et al.* 1987; Scott & Stevenson 1989; Turcotte & Phipps Morgan 1992; Scott 1992). Diapiric structures are observed in mantle from beneath a spreading ridge in the Oman ophiolite (Nicolas 1989; Ceuleneer & Rabinowicz 1992; Nicolas & Boudier 1995). However, some of types of focused solid flow are not viable in the sense that they produce liquids very different from MORB (Spiegelman 1996). In addition, Hirth & Kohlstedt (1996) suggest that – as a consequence of dehydration due to partial melting – mantle viscosities may be too high to produce buoyancy-driven flow strong enough to account for focusing of melt

to the ridge axis. In any case, melt flow in chemically isolated conduits is required to preserve disequilibrium between MORB and mantle peridotite (§ 1 *b*). Focused solid upwelling, combined with formation of flow channels, might account for melt focusing to ridge axes.

(*c*) *Coalescing dissolution channels? Maybe.*

As noted in § 2 *a* (vi), dissolution channels formed as a consequence of the RII may coalesce downstream where solubility of the solid matrix increases downstream. Aharonov *et al.* (1995) showed that, in the initial stages of the instability, the preferred wavelength in channel spacing increases with increasing permeability. Channels on a small scale may be regarded as 'pores' on a larger scale. Thus, the larger scale permeability is higher, and the preferred wavelength for channels may be larger. We inferred that this leads to coalescence of channels in time and in space. Initial results of numerical modelling of the RII, illustrated in figure 7, show coalescence in time and space. In these preliminary results, the spacing of the largest channels depends mainly on the compaction length (Spiegelman *et al.* 1996).

Can coalescence of channels formed by the RII lead to focused melt extraction beneath mid-ocean ridges? Maybe. At first, it seems unlikely, since the aspect ratio (height/width) for coalescence of channels in figure 7 is larger than 1, whereas the aspect ratio of the melting region must be close to 1 (Plank & Langmuir 1992). However, our preliminary numerical modelling has been in a static solid reference frame, whereas beneath a mid-ocean ridge, melt generated near the solidus rises into mantle in which a conduit geometry has already been established. There may be large, preexisting dissolution channels near the centre of the upwelling system that 'suck' melt inward. In addition, numerical modelling has been for dissolution reactions alone, so that porosities between channels become very small. With decompression melting as well as dissolution, lateral flow from one conduit into another may be facilitated by larger inter-channel porosities. For these reasons, lateral pressure gradients due to dissolution channels beneath mid-ocean ridges might lead to coalescence with smaller aspect ratios than in figure 7. Also, as noted in § 4 *d*, there may be several other causes of lateral pressure gradients which would enhance coalescence of a dissolution channel network.

Isotopic heterogeneity in MORB within a single ridge segment (Langmuir *et al.* 1992) indicates that a single network of coalescing conduits may not be sufficient to explain melt extraction. Instead, several networks might converge at the base of a ridge segment, each tapping spatially and chemically distinct domains within the upwelling mantle. Therefore, the aspect ratio of individual channel networks need not be (must not be?) as small as the aspect ratio of the entire melting regime, and additional factors must combine to ensure that all channel networks converge near the ridge axis.

(*d*) *Other mechanisms for lateral focusing of porous flow*

Sparks & Parmentier (1991), and Spiegelman (1993*c*) proposed that partial crystallization of melt rising into the conductively cooled lithosphere on either side of a ridge may create a permeability barrier that impedes vertical melt flow. Because the base of the lithosphere slopes upward toward the ridge axis, like a tent, ascending melt would migrate toward the ridge below the permeability barrier in a high porosity band. In its simplest form, this hypothesis is inconsistent with the geochemical constraints reviewed in §§ 1 *a*, *b*. All abyssal peridotite and ophiolite mantle must

pass through the roof of the tent. MORB and mantle peridotite would not preserve evidence for disequilibrium if solid flow lines all passed through a horizon in which aggregated, ascending melt was transported to the ridge axis. However, if combined with the presence of channels for chemically isolated melt flow within the roof, the tent mechanism could play a role in focusing melt to the ridge axis.

Phipps Morgan (1987) and Spiegelman & McKenzie (1987) showed that pressure gradients in viscously deforming peridotite undergoing corner flow might focus porous flow of melt toward a ridge axis. Required mantle viscosities, *ca.* 10^{20} Pa s, were higher than contemporary estimates of the viscosity of the mantle beneath ridge axes. However, a more recent viscosity estimate suggests that this process may be viable (Hirth & Kohlstedt 1996). Phipps Morgan (1987) also suggested that anisotropy in permeability might focus melt to the ridge axis. Field data from the Josephine peridotite confirm that melt does preferentially flow along the foliation in peridotites with a strong lattice preferred orientation (Kelemen & Dick 1995). Since diffuse porous flow cannot be the primary mode of MORB extraction from the mantle, this mechanism must be combined with the formation of chemically isolated conduits to explain magma transport beneath ridges.

5. Conclusion

For the moment, a clear picture has emerged for many aspects of melt extraction beneath ridges. Most melt is extracted from the adiabatically upwelling mantle by focused flow in dunite conduits; around these conduits, small amounts of melt migrate by reactive porous flow. The lowest pressure melts, 'ultra-depleted' liquids from the shallow mantle just beneath the conductive lithosphere, may be extracted primarily in fractures unrelated to dunite conduits.

Melt velocity constraints from U/Th isotope systematics can be satisfied by porous flow of melt from the base of the melting regime to the base of the crust. Provided that conduit porosities are larger than source porosities and melt-free mantle viscosities are less than *ca.* 10^{20} Pa s, flow in fractures is not required. Melt velocities of *ca.* 50 m yr^{-1} have been inferred from patterns of post-glacial volcanism and from ^{226}Ra excess. If these inferences are correct, the minimum conditions for hydrofracture may be reached in the upwelling mantle beneath ridges, even if mantle viscosities are less than *ca.* 10^{20} Pa s. Hydrofracture could arise periodically within coarse, high porosity dunite conduits, especially in the shallowest part of the melting region near the transition to conductively cooled lithosphere. Melt-filled tubes might also form in the asthenosphere by dissolution and/or mechanical instabilities within dunite conduits. If they form, fractures or tubes are probably closed at the top and bottom, and follow pre-existing dunites in order to maintain observed disequilibrium between MORB and shallow mantle peridotites. On a plate scale, focusing of melt flow toward ridges is best explained as a combination of porous flow mechanisms including the coalescence of dissolution channels, 'suction' of melt toward the ridge resulting from corner flow, flow along high permeability planes in foliated peridotite, and, perhaps, flow along a porous conduit beneath a permeability barrier near the base of the lithosphere.

There are several key areas of uncertainty regarding mechanisms of melt extraction. These include the relationship between permeability, porosity, and grain size in partially molten mantle peridotite, the tensile fracture strength of partially molten

peridotite, the extent and nature of 'near-fractional' melting processes, the depth of formation of ^{226}Ra isotopic disequilibrium, the proportion of melt extraction due to hydrofracture in the asthenosphere, and the factors governing the size, shape and fluid mechanics of melt-filled cracks or tubes in viscous, porous media. In addition, substantial insight can be expected as the grain scale kinetics of melt/rock interaction are more fully explored.

Our thanks to Joe Cann, who suggested that we write this paper, and to Adolphe Nicolas, Benoit Ildefonse, Françoise Boudier, Einat Aharonov, Ken Sims, Stan Hart, Lucy Slater, Dan McKenzie, Chris Richardson, Matthew Jull, Karl Gronvold, Uli Faul, Marc Hirschmann, Dave Scott, Jack Whitehead, Dave Kohlstedt, Martha Daines, Brian Evans, Ed Stolper, and Kent Ross for advice, encouragement, reviews, and access to unpublished manuscripts. Work on this paper and collection of previously unpublished data were supported by US National Science Foundation grants OCE-9314013, OCE-9416616 and EAR-9418228 (P.B.K.), and EAR-9405845 (G.H.).

References

Aharonov, E., Whitehead, J. A., Kelemen, P. B. & Spiegelman, M. 1995 Channeling instability of upwelling melt in the mantle. *J. Geophys. Res.* **100**, 20 433–20 450.

Alabaster, T., Pearce, J. A. & Malpas, J. 1982 The volcanic stratigraphy and petrogenesis of the Oman ophiolite complex. *Contrib. Mineral. Petrol.* **81**, 168–183.

Allan, J. F. & Dick, H. J. B 1996 Cr-rich spinel as a tracer for melt migration and melt-wall rock interaction in the mantle: Hess Deep, Leg 147. *Sci. Res. Ocean Drill. Prog.* **147**, 157–172.

Allègre, C. J., Montigny, R. & Bottinga, Y. 1973 Cortège ophiolitique et cortège océanique, géochimie comparée et mode de genèse. *Bull. Soc. géol. France* **15**, 461–477.

Arai, S. & Matsukage, K. 1996 Petrology of gabbro-troctolite-peridotite complex from Hess Deep, Equatorial Pacific: implications for mantle-melt interaction within the oceanic lithosphere. *Sci. Res. Ocean Drill. Prog.* **147**, 135–155.

Asimow, P. D., Hirschmann, M. M., Ghiorso, M. S., O'Hara, M. J. & Stolper, E. M. 1995 The effect of pressure-induced solid–solid phase transitions on decompression melting of the mantle. *Geochim. Cosmochim. Acta* **59**, 4489–4506.

Augé, T. 1987 Chromite deposits in the northern Oman ophiolite: mineralogical constraints. *Mineral. Deposita* **22**, 1–10.

Beattie, P. 1993*a* The generation of uranium series disequilibria by partial melting of spinel peridotite: constraints from partitioning studies. *Earth Planet. Sci. Lett.* **117**, 379–391.

Beattie, P. 1993*b* Uranium–thorium disequilibria and partitioning on melting of garnet peridotite. *Nature* **363**, 63–65.

Benoit, M., Polvé, M. & Ceuleneer, G. 1997 Trace element and isotopic characterization of mafic cumulates in a fossil mantle diapir (Oman ophiolite). *Chem. Geol.* (In the press.)

Berger, E. T. & Vannier, M. 1984 Les dunites en enclaves dans les basaltes alcalins des iles océaniques: approche pétrologique. *Bull. Miner.* **107**, 649–663.

Beeman, M. L. & Kohlstedt, D. L. 1992 Deformation of fine-grained aggregates of olivine plus melt at high temperatures and pressures. *J. Geophys. Res.* **98**, 6443–6452.

Bodinier, J. L. 1988 Geochemistry and petrogenesis of the Lanzo peridotite body, Western Alps. *Tectonophysics* **149**, 67–88.

Bodinier, J. L., Vasseur, G., Vernieres, J., Dupuy, C. & Fabries, J. 1990 Mechanisms of mantle metasomatism: geochemical evidence from the Lherz orogenic peridotite. *J. Petrol.* **31**, 597–628.

Boudier, F. & Coleman, R. G. 1981 Cross section through the peridotite in the Samail Ophiolite, southeastern Oman Mountains. *J. Geophys. Res.* **86**, 2573–2592.

Boudier, F. & Nicolas, A. 1972 Fusion partielle gabbroique dans la Iherzolite de Lanzo. *Bull. Suisse Min. Pet.* **52**, 39–56.

Boudier, F. & Nicolas, A. 1995 Nature of the Moho Transition Zone in the Oman ophiolite. *J. Petrol.* **36**, 777–796.

Bussod, G. Y. & Christie, J. M. 1991 Textural development and melt topology in spinel lherzolite experimentally deformed at hypersolidus conditions. *J. Petrol.* (Special Lherzolite Issue), pp. 17–39.

Cannat, M. 1996 How thick is the magmatic crust at slow spreading oceanic ridges? *J. Geophys. Res.* **101**, 2847–2857.

Cannat, M. & Casey, J. F. 1995 An ultramafic lift at the Mid-Atlantic Ridge: successive stages of magmatism in serpentinized peridotites from the 15° N region. In *Mantle and lower crust exposed in oceanic ridges and in ophiolites* (ed. R. L. M. Vissers & A. Nicolas), pp. 5–34. Amsterdam: Kluwer.

Ceuleneer, G. & Rabinowicz, M. 1992 Mantle flow and melt migration beneath oceanic ridges: models derived from observations in ophiolites. *Geophys. Monograph* **71**, 123–154.

Chadam, J., Hoff, D., Merino, E., Ortoleva, P. & Sen, A. 1986 Reactive infiltration instabilities. *J. Appl. Math.* **36**, 207–221.

Cheadle, M. J. 1993 The physical properties of texturally equilibrated partially molten rocks. *Eos* **74**, 283.

Chopra, P. N. & Paterson, M. S. 1984 The role of water in the deformation of dunite. *J. Geophys. Res.* **89**, 7861–7876.

Crane, K. 1985 The spacing of rift axis highs: dependence upon diapiric processes in the underlying asthenosphere? *Earth Planet. Sci. Lett.* **72**, 405–414.

Daccord, G. 1987 Chemical dissolution of a porous medium by a reactive fluid. *Phys. Rev. Lett.* **58**, 479–482.

Daccord, G. & Lenormand, R. 1987 Fractal patterns from chemical dissolution. *Nature* **325**, 41–43.

Daines, M. J. & Kohlstedt, D. L. 1993 A laboratory study of melt migration. *Phil. Trans. R. Soc. Lond.* A **342**, 43–52.

Daines, M. J. & Kohlstedt, D. L. 1994 The transition from porous to channelized flow due to melt/rock reaction during melt migration. *Geophys. Res. Lett.* **21**, 145–148.

DePaolo, D. J. 1981 Trace element and isotopic effects of combined wallrock assimilation and fractional crystallization. *Earth Planet. Sci. Lett.* **53**, 189–202.

Dick, H. J. B. 1976 The origin and emplacement of the Josephine peridotite of Southwestern Oregon. Ph.D. thesis, Yale University, New Haven, NJ, USA.

Dick, H. J. B. 1977 Evidence for partial melting in the Josephine peridotite. *Bull. Oregon St. Dept. Geol. Miner. Ind.* **96**, 63–78.

Dick, H. J. B. 1989 Abyssal peridotites, very slow spreading ridges and ocean ridge magmatism. In *Magmatism in the ocean basins* (ed. A. D. Saunder & M. J. Norry), pp. 71–105. Geological Society Special Publications.

Dick, H. J. B. & Bullen, T. 1984 Chromian spinel as a petrogenetic indicator in abyssal and alpine-type peridotites and spatially associated lavas. *Contrib. Mineral. Petrol.* **86**, 54–76.

Dick, H. J. B. & Natland, J. H. 1996 Late stage melt evolution and transport in the shallow mantle beneath the East Pacific Rise. *Sci. Res. Ocean Drill. Prog.* **147**, 103–134.

Elthon, D. & Scarfe, C. M. 1980 High-pressure phase equilibria of a high-magnesia basalt: implications for the origin of mid-ocean ridge basalts. *Carnegie Inst. Wa. Yrbk*, pp. 277–281.

Elthon, D. 1992 Chemical trends in abyssal peridotites: refertilization of depleted suboceanic mantle. *J. Geophys. Res.* **97**, 9015–9025.

Farrier, K., Kelemen, P. B. & Shimizu, N. 1997 Off-axis gabbro and pyroxenite dikes in the Oman ophiolite: transport of ultra-depleted melts in lithospheric fractures. (In preparation.)

Faul, U. H. 1997 The permeability of partially molten upper mantle rocks from experiments and percolation theory. *J. Geophys. Res.* (In the press.)

Forsyth, D. W. 1992 Geophysical constraints on mantle flow and melt generation beneath mid-ocean ridges. *Geophys. Monograph* **71**, 1–65.

Forsyth, D. W. 1996 Partial melting beneath a Mid-Atlantic Ridge segment detected by teleseismic PKP delays. *Geophys. Res. Lett.* **23**, 463–466.

Fowler, A. C. & Scott, D. R. 1997 Hydraulic crack propagation in a porous medium. *Geophys. J. Int.* (In the press.)

Gaetani, G. A., DeLong, S. E. & Wark, D. A. 1995 Petrogenesis of basalts from the Blanco Trough, northeast Pacific: inferences for off-axis melt generation. *J. Geophys. Res.* **100**, 4197–4214.

Gast, P. W. 1968 Trace element fractionation and the origin of tholeiitic and alkaline magma types. *Geochim. Cosmochim. Acta* **32**, 1057–1089.

Gruau, G., Bernard-Griffiths, J., Lecuyer, C., Henin, O., Mace, J. & Cannat, M. 1995 Extreme Nd isotopic variation in the Trinity ophiolite complex and the role of melt/rock reactions in the oceanic lithosphere. *Contrib. Mineral. Petrol.* **121**, 337–350.

Gregory, R. T. 1984 Melt percolation beneath a spreading ridge: evidence from the Semail peridotite, Oman. *Geol. Soc. Lond. Spec. Publ.* **13**, 55–62.

Hager, B. H. 1991 Mantle viscosity: a comparison of models from postglacial rebound and from the geoid, plate driving forces, and advected heat flux. In *Glacial isostasy, sea-level and mantle rheology* (ed. R. Sabadini *et al.*), pp. 493–513. Dordrecht: Kluwer Academic.

Hart, S. R. 1993 Equilibrium during mantle melting: a fractal tree model. *Proc. Natn. Acad. Sci.* **90**, 11914–11918.

Hart, S. R. & Dunn, T. 1993 Experimental cpx/melt partitioning of 24 trace elements. *Contrib. Mineral. Petrol.* **113**, 1–8.

Hirschmann, M. M. & Stolper, E. M. 1996 A possible role for garnet pyroxenite in the origin of the garnet signature in MORB. *Contrib. Mineral. Petrol.* **124**, 185–208.

Hirth, G. & Kohlstedt, D. L. 1995 Experimental constraints on the dynamics of the partially molten upper mantle. 2. Deformation in the dislocation creep regime. *J. Geophys. Res.* **100**, 15 441–15 449.

Hirth, G. & Kohlstedt, D. L. 1995 Experimental constraints on the dynamics of the partially molten upper mantle: deformation in the diffusion creep regime. *J. Geophys. Res.* **100**, 1981–2001.

Hirth, G. & Kohlstedt, D. L. 1996 Water in the oceanic mantle: implications for rheology, melt extraction, and the evolution of the lithosphere. *Earth Planet. Sci. Lett.* **144**, 93–108.

Hoefner, M. L. & Fogler, H. S. 1988 Pore evolution and channel formation during flow and reaction in porous media. *AlChE Jl* **34**, 45–54.

Hopson, C. A., Coleman, R. G., Gregory, R. T., Pallister, J. S. & Bailey, E. H. 1981 Geologic section through the Samail Ophiolite and associated rocks along a Muscat-Ibra Transect, Southeastern Oman Mountains. *J. Geophys. Res.* **86**, 2527–2544.

Iwamori, H. 1993 A model for disequilibrium mantle melting incorporating melt transport by porous and channel flows. *Nature* **366**, 734–737.

Iwamori, H. 1994 $^{238}U/^{230}Th/^{226}Ra$ and $^{235}U/^{231}Pa$ disequilibria produced by mantle melting with porous and channel flows. *Earth Planet. Sci. Lett.* **125**, 1–16.

Jin, Z.-M., Green, H. W. & Zhou, Y. 1994 Melt topology in partially molten mantle peridotite during ductile deformation. *Nature* **372**, 164–167.

Johnson, K. T. M. & Dick, H. J. B. 1992 Open system melting and temporal and spatial variation of peridotite and basalt at the Atlantis II Fracture Zone. *J. Geophys. Res.* **97**, 9219–9241.

Johnson, K. T. M., Dick, H. J. B. & Shimizu, N. 1990 Melting in the oceanic upper mantle: an ion microprobe study of diopsides in abyssal peridotites. *J. Geophys. Res.* **95**, 2661–2678.

Jull, M. & McKenzie, D. 1996 The effect of deglaciation on mantle melting beneath Iceland. *J. Geophys. Res.* **101**, 21 815–21 828.

Kelemen, P. B. 1990 Reaction between ultramafic rock and fractionating basaltic magma. I. Phase relations, the origin of calc-alkaline magma series, and the formation of discordant dunite, *J. Petrol.* **31**, 51–98.

Kelemen, P. B. & Dick, H. J. B. 1995 Focused melt flow and localized deformation in the upper mantle: juxtaposition of replacive dunite and ductile shear zones in the Josephine peridotite, SW Oregon. *J. Geophys. Res.* **100**, 423–438.

Kelemen, P. B., Dick, H. J. B. & Quick, J. E. 1992 Formation of harzburgite by pervasive melt/rock reaction in the upper mantle. *Nature* **358**, 635–641.

Kelemen, P. B., Whitehead, J. A., Aharonov, E. & Jordahl, K. A. 1995*a* Experiments on flow focusing in soluble porous media, with applications to melt extraction from the mantle. *J. Geophys. Res.* **100**, 475–496.

Kelemen, P. B., Shimizu, N. & Salters, V. J. M. 1995*b* Extraction of mid-ocean-ridge basalt from the upwelling mantle by focused flow of melt in dunite channels. *Nature* **375**, 747–753.

Kelemen, P.B., Koga, K. & Shimizu, N. 1997 Geochemistry of gabbro sills in the crust/mantle transition zone of the Oman ophiolite: implications for the origin of the oceanic lower crust. *Earth Planet. Sci. Lett.* (In the press.)

Kinzler, R. J. & Grove, T. L. 1992 Primary magmas of mid-ocean ridge basalts. 2. Applications. *J. Geophys. Res.* **97**, 6907–6926.

Klein, E. & Langmuir, C. H. 1987 Global correlations of ocean ridge basalt chemistry with axial depth and crustal thickness. *J. Geophys. Res.* **92**, 8089–8115.

Kushiro, I. 1986 Viscosity of partial melts in the upper mantle. *J. Geophys. Res.* **91**, 9343–9350.

Lago, B. L., Rabinowicz, M. & Nicolas, A. 1982 Podiform chromite ore bodies: a genetic model. *J. Petrol.* **23**, 103–125.

Langmuir, C. H., Bender, J. F., Bence, A. E., Hanson, G. N. & Taylor, S. R. 1977 Petrogenesis of basalts from the Famous area, Mid-Atlantic Ridge. *Earth Planet. Sci. Lett.* **36**, 133–156.

Leblanc, M. & Ceuleneer, G. 1992 Chromite crystallization in a multicellular magma flow: evidence from a chromitite dike in the Oman ophiolite. *Lithos* **27**, 231–257.

Lippard, S. J., Shelton, A. W. & Gass, I. G. 1986 *The ophiolite of northern Oman.* (178 pages.) Oxford: Blackwell.

Lundstrom, C. C., Gill, J., Williams, Q. & Perfit, M. R. 1995 Mantle melting and basalt extraction by equilibrium porous flow. *Science* **270**, 1958–1961.

Maaloe, S. 1981 Magma accumulation in the ascending mantle. *J. Geol. Soc. Lond.* **138**, 223–236.

Maaloe, S. & Scheie, A. 1982 The permeability controlled accumulation of primary magma. *Contrib. Mineral. Petrol.* **81**, 350–357.

Magde, L. S., Detrick, R. S. & the TERA Group 1995 Crustal and upper mantle contribution to the axial gravity anomaly at the southern East Pacific Rise. *J. Geophys. Res.* **100**, 3747–3766.

McKenzie, D. 1984 The generation and compaction of partially molten rock. *J. Petrol.* **25**, 713–765.

McKenzie, D. 1985 ^{230}Th–^{238}U disequilibrium and the melting processes beneath ridge axes. *Earth Planet. Sci. Lett.* **72**, 149–157.

McKenzie, D. 1987 The compaction of igneous and sedimentary rocks. *J. Geol. Soc. Lond.* **144**, 299–307.

McKenzie, D. 1989 Some remarks on the movement of small melt fractions in the mantle. *Earth Planet. Sci. Lett.* **95**, 53–72.

McKenzie, D. & Bickle, M. J. 1988 The volume and composition of melt generated by extension of the lithosphere. *J. Petrol.* **29**, 625–679.

Menzies, M., Kempton, P. & Dungan, M. 1985 Interaction of continental lithosphere and asthenospheric melts below the Geronimo Volcanic Field, Arizona, U.S.A. *J. Petrol.* **26**, 663–693.

Mercier, J.-C. 1980 Magnitude of the continental lithospheric stresses inferred from rheomorphic petrology. *J. Geophys. Res.* **85**, 6293–6303.

Nicolas, A. 1986 A melt extraction model based on structural studies in mantle peridotites. *J. Petrol.* **27**, 999–1022.

Nicolas, A. 1989 *Structures of ophiolites and dynamics of oceanic lithosphere.* (367 pages.) Dordrecht: Kluwer Academic.

Nicolas, A. 1990 Melt extraction from mantle peridotites: hydrofracturing and porous flow, with consequences for oceanic ridge activity. In *Magma transport and storage* (ed. M. P. Ryan), pp. 159–174. New York: Wiley.

Nicolas, A. & Boudier, F. 1995 Mapping oceanic ridge segments in Oman ophiolite. *J. Geophys. Res.* **100**, 6179–6197.

Niu, Y. & Batiza, R. 1993 Chemical variation trends at fast and slow spreading mid-ocean ridges. *J. Geophys. Res.* **98**, 7887–7902.

O'Hara, M. J. 1965 Primary magmas and the origin of basalts. *Scot. J. Geol.* **1**, 19–40.

Ozawa, K. 1994 Melting and melt segregation in the mantle wedge above a subduction zone: evidence from the chromite-bearing peridotites of the Miyamori ophiolite complex, northeastern Japan. *J. Petrol.* **35**, 647–678.

PHILOSOPHICAL TRANSACTIONS OF THE ROYAL SOCIETY A MATHEMATICAL, PHYSICAL & ENGINEERING SCIENCES

Ozawa, K. & Shimizu, N. 1995 Open-system melting in the upper mantle: constraints from the Miyamori–Hayachine ophiolite, northeastern Japan. *J. Geophys. Res.* **100**, 22 315–22 335.

Pallister, J. S. & Hopson, C. A. 1981 Samail ophiolite plutonic suite: field relations, phase variation, cryptic variation and layering, and a model of a spreading ridge magma chamber. *J. Geophys. Res.* **86**, 2593–2644.

Paterson, M. S. 1978 *Experimental rock deformation: the brittle field.* (254 pages.) Berlin: Springer.

Phipps Morgan, J. 1987 Melt migration beneath mid-ocean spreading centers. *Geophys. Res. Let.* **14**, 1238–1241.

Plank, T. & Langmuir, C. H. 1992 Effects of the melting regime on composition of the oceanic crust. *J. Geophys. Res.* **97**, 19 749–19 770.

Quick, J. E. 1981*a* Petrology and petrogenesis of the Trinity peridotite, an upper mantle diapir in the eastern Klamath Mountains, Northern California. *J. Geophys. Res.* **86**, 11 837–11 863.

Quick, J. E. 1981*b* The origin and significance of large, tabular dunite bodies in the Trinity peridotite, Northern California. *Contrib. Mineral. Petrol.* **78**, 413–422.

Quick, J. E. & Gregory, R. T. 1995 Significance of melt-wall rock reaction: a comparative anatomy of three ophiolites. *J. Geol.* **103**, 187–198.

Rabinowicz, M., Ceuleneer, G. & Nicolas, A. 1987 Melt segregation and flow in mantle diapirs below spreading centers: evidence from the Oman ophiolite. *J. Geophys. Res.* **92**, 3475–3486.

Richardson, C. N. & McKenzie, D. 1984 Radioactive disequilibria from 2D models of melt generation by plumes and ridges. *Earth Planet. Sci. Lett.* **128**, 425–437.

Richardson, C. N., Lister, J. R. & McKenzie, D. 1996 Melt conduits in a viscous porous matrix. *J. Geophys. Res.* **101**, 20 423–20 432.

Riley Jr, G. N. & Kohlstedt, D. L. 1991 Kinetics of melt migration in upper mantle-type rocks. *Earth Planet. Sci. Lett.* **105**, 500–521.

Ross, K. & Elthon, D. 1993 Cumulates from strongly depleted mid-ocean ridge basalts. *Nature* **365**, 826–829.

Ross, K. & Elthon, D. 1997*a* Cumulus and post-cumulus crystallization in the oceanic crust: major and trace element geochemistry of Leg 153 gabbroic rocks. *Scientific results of the Ocean Drilling Program* **153**. (In the press.)

Ross, K. & Elthon, D. 1997*b* Extreme incompatible trace element depletion of diopside in residual mantle from south of the Kane Fracture Zone. *Scientific Results of the Ocean Drilling Program* **153**. (In the press.)

Salters, V. J. M. & Hart, S. R. 1989 The hafnium paradox and the role of garnet in the source of mid-ocean-ridge basalts. *Nature* **342**, 420–422.

Scholz, C. H. 1990 *The mechanics of earthquakes and faulting.* (439 pages.) Cambridge University Press.

Scott, D. R. 1992 Small-scale convection and mantle melting beneath mid-ocean ridges. *Geophys. Monograph* **71**, 327–352.

Scott, D. R. & Stevenson, D. J. 1989 A self-consistent model of melting, magma migration and buoyancy-driven circulation beneath mid-ocean ridges. *J. Geophys. Res.* **94**, 2973–2988.

Shaw, D. M. 1970 Trace element fractionation during anatexis. *Geochim. Cosmochim. Acta* **34**, 237–243.

Shimizu, N. 1997 The geochemistry of olivine-hosted melt inclusions in FAMOUS basalt ALV519-4-1. *Phys. Earth Planet. Int.* (In the press.)

Sims, K. W. W., DePaolo, D. J., Murrell, M. T., Baldridge, W. S., Goldstein, S. J. & Clague, D. A. 1995 Mechanisms of magma generation beneath Hawaii and mid-ocean ridges: uranium/thorium and samarium/neodymium isotopic evidence. *Science* **267**, 508–512.

Sleep, N. H. 1975 Formation of oceanic crust: some thermal constraints. *J. Geophys. Res.* **80**, 4037–4042.

Sleep, N. H. 1984 Tapping of magmas from ubiquitous mantle heterogeneities: an alternative to mantle plumes? *J. Geophys. Res.* **89**, 10 029–10 041.

Sleep, N. H. 1988 Tapping of melt by veins and dikes. *J. Geophys. Res.* **93**, 10 255–10 272.

Sparks, D. W. & Parmentier, E. M. 1991 Melt extraction from the mantle beneath mid-ocean ridges. *Earth Planet. Sci. Lett.* **105**, 368–377.

Spera, F. J. 1980 Aspects of magma transport. In *Physics of magmatic processes* (ed. R. B. Hargraves), pp. 263–323. Princeton University Press.

Spiegelman, M. 1993*a* Flow in deformable porous media. 1. Simple analysis. *J. Fluid Mech.* **247**, 17–38.

Spiegelman, M. 1993*b* Flow in deformable porous media. 2. Numerical analysis – the relationship between shock waves and solitary waves. *J. Fluid Mech.* **247**, 39–63.

Spiegelman, M. 1993*c* Physics of melt extraction: theory, implications and applications. *Phil. Trans. R. Soc. Lond.* A **342**, 23–41.

Spiegelman, M. 1996 Geochemical consequences of melt transport in 2-D: the sensitivity of trace elements to mantle dynamics. *Earth Planet. Sci. Lett.* **139**, 115–132.

Spiegelman, M. & Elliot, T. 1993 Consequences of melt transport for uranium series disequilibrium. *Earth Planet. Sci. Lett.* **118**, 1–20.

Spiegelman, M. & Kenyon, P. 1992 The requirements for chemical disequilibrium during magma migration. *Earth Planet. Sci. Lett.* **109**, 611–620.

Spiegelman, M. & McKenzie, D. 1987 Simple 2-D models for melt extraction at mid-ocean ridges and island arcs. *Earth Planet. Sci. Lett.* **83**, 137–152.

Spiegelman, M., Aharonov, E. & Kelemen, P. B. 1996 The compaction reaction: magma channel formation by reactive flow in deformable media. *Eos* **77**, F783.

Sobolev, A. V. 1997 Melt inclusions in minerals as a source of principal petrologic information. *Petrology* **4**. (In the press.)

Sobolev, A. V. & Shimizu, N. 1993 Ultra-depleted primary melt included in an olivine from the Mid-Atlantic Ridge. *Nature* **363**, 151–154.

Sobolev, A. V. & Shimizu, N. 1994 The origin of typical N-MORB: the evidence from a melt inclusion study. *Min. Mag.* A **58**, 862–863.

Stolper, E. 1980 A phase diagram for mid-ocean ridge basalts: preliminary results and implications for petrogenesis. *Contrib. Mineral. Petrol.* **74**, 13–27.

Stevenson, D. J. 1989 Spontaneous small-scale melt segregation in partial melts undergoing deformation. *Geophys. Res. Lett.* **16**, 1067–1070.

Tait, S., Jahrling, K. & Jaupart, C. 1992 The planform of compositional convection and chimney formation in a mushy layer. *Nature* **359**, 406–408.

Takahashi, N. 1992 Evidence for melt segregation towards fractures in the Horoman mantle peridotite complex. *Nature* **359**, 52–55.

Takazawa, E. 1996 Geodynamic evolution of the Horoman peridotite, Japan: consequence of lithospheric and asthenospheric processes. (562 pp.) Ph.D. thesis, MIT.

Takazawa, E., Frey, F. A., Shimizu, N., Obata, M. & Bodinier, J. L. 1992 Geochemical evidence for melt migration and reaction in the upper mantle. *Nature* **359**, 55–58.

Toramaru, A. & Fujii, N. 1986 Connectivity of melt phase in a partially molten peridotite. *J. Geophys. Res.* **91**, 9239–9252.

Tilton, G. R., Hopson, C. A. & Wright, J. E. 1981 Uranium-lead isotopic ages of the Samail ophiolite, Oman, with applications to Tethyan ocean ridge tectonics. *J. Geophys. Res.* **86**, 2763–2775.

Turcotte, D. L. & Phipps Morgan, J. 1992 The physics of magma migration and mantle flow beneath a mid-ocean ridge. *Geophys. Monograph* **71**, 155–182.

Von Bargen, N. & Waff, H. S. 1986 Permeabilities, interfacial areas and curvatures of partially molten systems: results of numerical computations of equilibrium microstructures. *J. Geophys. Res.* **91**, 9261–9276.

Waff, H. S. & Bulau, J. R. 1979 Equilibrium fluid distribution in an ultramafic partial melt under hydrostatic stress conditions. *J. Geophys. Res.* **84**, 6109–6114.

Waff, H. S. & Faul, U. H. 1992 Effects of crystalline anisotropy on fluid distribution in ultramafic partial melts. *J. Geophys. Res.* **97**, 9003–9014.

Wang, H. F. 1993 A double medium model for diffusion in fluid-bearing rock. *Contrib. Mineral. Petrol.* **114**, 357–364.

Wang, Y. & Merino, E. 1993 Oscillatory magma crystallization by feedback between the concentrations of the reactant species and mineral growth rates. *J. Petrol.* **34**, 369–382.

Wang, Y. & Merino, E. 1995 Origin of fibrosity and banding in agates from flood basalts. *Am. Jl Sci.* **295**, 49–77.

Whitehead, J. A., Dick, H. J. B. & Schouten, H. 1984 A mechanism for magmatic accretion under spreading centres. *Nature* **312**, 146–148.

Williams, R. W. & Gill, J. B. 1989 Effects of partial melting on the uranium decay series. *Geochim. Cosmochim. Acta* **53**, 1607–1619.

Wiggins, C. & Spiegelman, M. 1995 Magma migration and magmatic solitary waves in 3-D. *Geophys. Res. Lett.* **22**, 1289–1292.

PHILOSOPHICAL TRANSACTIONS OF THE ROYAL SOCIETY A MATHEMATICAL, PHYSICAL & ENGINEERING SCIENCES